Leptogenesis, primordial gravitational waves, and PBH-induced reheating

Basabendu Barman ,[1,*] Suruj Jyoti Das ,[2,†] Md Riajul Haque ,[3,‡] and Yann Mambrini[4,§]

[1]*Department of Physics, School of Engineering and Sciences, SRM University-AP, Amaravati 522240, India*

[2]*Particle Theory and Cosmology Group, Center for Theoretical Physics of the Universe, Institute for Basic Science (IBS), Daejeon 34126, Korea*

[3]*Centre for Strings, Gravitation, and Cosmology, Department of Physics, Indian Institute of Technology Madras, Chennai 600036, India*

[4]*Université Paris-Saclay, CNRS/IN2P3, IJCLab, 91405 Orsay, France*

(Received 18 March 2024; accepted 31 July 2024; published 26 August 2024)

We explore the possibility of producing the observed matter-antimatter asymmetry of the Universe uniquely from the evaporation of primordial black holes (PBHs) that are formed in an inflaton-dominated background. Considering the inflaton (ϕ) to oscillate in a monomial potential $V(\phi) \propto \phi^n$, we show, it is possible to obtain the desired baryon asymmetry via vanilla leptogenesis from evaporating PBHs of initial mass $\lesssim 10$ g. We find that the allowed parameter space is heavily dependent on the shape of the inflaton potential during reheating (determined by the exponent of the potential n), the energy density of PBHs (determined by β), and the nature of the coupling between the inflaton and the Standard Model. To complete the minimal gravitational framework, we also include in our analysis the gravitational leptogenesis setup through inflaton scattering via exchange of graviton, which opens up an even larger window for PBH mass, depending on the background equation of state. We finally illustrate that such gravitational leptogenesis scenarios can be tested with upcoming gravitational wave (GW) detectors, courtesy of the blue-tilted primordial GW with inflationary origin, thus paving a way to probe a PBH-induced reheating together with leptogenesis.

DOI: 10.1103/PhysRevD.110.043528

I. INTRODUCTION

Initially proposed by Stephen Hawking and Bernard Carr, primordial black holes (PBHs) exhibit captivating cosmic signatures [1,2]. PBHs with masses $M_{\rm BH} \gtrsim 10^{15}$ g remain stable at the present day and can be suitable for dark matter (DM) candidates (see, for example, Ref. [3] for a review). On the other side of the spectrum, the black holes must be much lighter to explore particle production from evaporating PBHs. Indeed, the formation mass should be within a range allowing for evaporation before big bang nucleosynthesis (BBN), corresponding to $M_{\rm BH} \lesssim 10^9$ g. Failure to meet this criterion could introduce additional degrees of freedom, potentially disrupting the successful prediction of BBN from the accurate measurement of $\Delta N_{\rm eff}$ [4]. Within this mass range, PBHs can undergo decay and play a central role in producing Standard Model (SM) particles, DM, and baryon asymmetry. Various studies that have explored DM production [5–35], baryon asymmetry [1,5,30,36–51] or cogenesis [5,13,15,24,25,39,41,43,44,52–55] from PBH evaporation, have consistently focused on PBH formation during standard radiation domination, overlooking the evolution of PBHs in a cosmological background dominated by the inflaton field.[1] However, recently, the authors of [58,59] studied the aftermath of PBH formation and evaporation during reheating, in presence of the inflaton field. They focused mainly on the production of DM relic from Schwarzschild BH and the effect of PBH decay on the reheating temperature. From these studies it was established that (a) the inflaton decay is more efficient at the beginning of the reheating process, whereas the evaporation of PBHs is more efficient at the end of their lifetime, and (b) PBH evaporation in an inflaton-dominated Universe can produce the entire observed DM relic abundance and even dominate the reheating process. Combining these two

*Contact author: basabendu.b@srmap.edu.in
†Contact author: surujjd@gmail.com
‡Contact author: riaj.0009@gmail.com
§Contact author: yann.mambrini@ijclab.in2p3.fr

[1]For the effect of reheating on flavor leptogenesis, see, for instance, Refs. [56,57].

natural sources (PBH and inflaton) of radiation and dark matter reopened a large part of the parameter space, which was forbidden.

If PBHs can greatly influence the production of particles in the early Universe still dominated with the inflaton field, it is natural to ask about the generation of baryon asymmetry through their evaporation within the epoch of reheating. As we know, an elegant mechanism to produce the baryon asymmetry of the Universe (BAU) is via leptogenesis [60,61], where a lepton asymmetry is generated first and subsequently gets converted into baryon asymmetry via nonperturbative sphaleron transitions [62]. In standard thermal leptogenesis [63–66], the decaying particles, typically right-handed neutrinos (RHNs), are produced thermally from the SM bath. However, the lower bound on the RHN mass in such scenarios (known as the Davidson-Ibarra bound), leads to a lower bound on the reheating temperature $T_{\rm RH} \gtrsim 10^{10}$ GeV [67], leading to the so-called "gravitino problem" [61,68]. A simple alternative to circumvent this, is to consider nonthermal production of RHNs [69–74], that can be sourced by the PBH evaporation.

On the other hand, there also exists an unavoidable production of RHNs through the gravitational interaction [75,76]. Indeed, it was shown in [77,78] that the transfer of energy from the inflaton background field can produce RHNs via the exchange of a massless graviton and is a valid source of BAU[2] and in another possibility, decay of those gravitationally produced RHNs may lead to the radiation dominated universe [82]. Therefore, this coupling being unavoidable makes it impossible to ignore the production of RHNs from the scattering of inflaton condensate, mediated by massless gravitons. In the present setup, we consider both contributions, namely, asymmetry from PBH evaporation and also from the graviton-mediated process, trying to combine both sources and find in which part of the parameter space one of the source dominates over the other one.

It is also important to note that for inflaton oscillating in a monomial potential $V(\phi) \propto \phi^n$ where the equation of state (EOS) is given by $w_\phi = (n-2)/(n+2)$, the value $w_\phi > 1/3$ (equivalently, $n > 4$) plays a crucial role in probing the reheating scenario with primordial GWs (PGW),[3] that are originated from the tensor fluctuations during inflation. Such a stiff period in the expansion history significantly enhances the inflationary GW background, making the corresponding signal potentially observable at several GW experimental facilities [84–103]. In the present context, the blue-tilted GW spectrum turns out to be well within the reach of several future GW detectors. More importantly, the red-tilted spectrum due to intermediate PBH-domination also turns out to be potentially detectable in detectors like BBO [104,105] and DECIGO [106,107]. This paves a way to testability of the present scenario, where any future detection can not only validate the inflationary paradigm but also hint towards a nontrivial cosmological history of the Universe prior to the onset of BBN.

The paper is organized as follows. After computing the BAU generated by PBH decay in the presence of the inflaton field in Sec. II, we compare it with the asymmetry produced through gravitational interaction in Sec. III. We then analyze possible GW signatures of our scenario in Sec. IV, before concluding.

A. Guide to scale-factor notations

$a_{\rm end}$: Scale factor at the end of inflation.
$a_{\rm in}$: Scale factor at PBH formation.
$a_{\rm BH}$: Scale factor at the onset of PBH domination.
$a_{\rm ev}$: Scale factor at PBH evaporation.
$a_{\rm RH}$: Scale factor at the end of reheating.

II. LEPTOGENESIS FROM PBH

A. Generalities

Assuming that PBHs have been formed during the reheating phase, their mass is typically related to the energy enclosed in the particle horizon. The mass $M_{\rm in}$ at formation time is given by [108]

$$M_{\rm in} = \frac{4}{3}\pi\gamma H_{\rm in}^{-3}\rho_\phi(a_{\rm in}) = 4\pi\gamma M_P^2 H_{\rm in}^{-1}, \tag{1}$$

where $\gamma = w_\phi^{3/2}$ parametrizes the efficiency of the collapse to form PBHs and $M_P = 1/\sqrt{8\pi G_N} \simeq 2.4 \times 10^{18}$ GeV is the reduced Planck mass.[4] $\rho_\phi(a_{\rm in})$ and $H_{\rm in}$ are the inflaton energy density and Hubble parameter, respectively, at the time of formation corresponding to the scale factor $a_{\rm in}$. In addition, the PBH mass evolves as [see Eq. (A1) in Appendix A]

$$M_{\rm BH}(t) = M_{\rm in}(1 - \Gamma_{\rm BH}(t - t_{\rm in}))^{\frac{1}{3}}, \tag{2}$$

where

$$\Gamma_{\rm BH} = 3\epsilon \frac{M_P^4}{M_{\rm in}^3}, \tag{3}$$

with $t_{\rm in}$ being the time of the formation and

$$\epsilon = \mathcal{G} \times \frac{\pi g_*(T_{\rm BH})}{480}, \tag{4}$$

[2]Such gravitational interaction can also reheat the Universe via gravitational reheating [79–81].
[3]For other relevant sources of PGW see, for example, the recent review [83].

[4]We can always choose a formation mechanism other than the horizon collapse, where the formation mass will differ. However, once we fixed the formation mass, the rest of the analysis related to reheating and leptogenesis via PBH-inflaton interplay remains as it is.

where $\mathcal{G} = 27/4$ is the graybody factor [109].[5] In the case of a Schwarzschild BH, which we will consider in the rest of our analysis, its temperature $T_{\rm BH}$ is related to its mass via [2]

$$T_{\rm BH} = M_P^2/M_{\rm BH}. \tag{5}$$

Finally, the PBH mass can not take arbitrary values. It is bounded from above and below within the window

$$1\ {\rm g} \lesssim M_{\rm in} \lesssim 10^8\ {\rm g}, \tag{6}$$

where the lower bound arises from the size of the horizon at the end of inflation $M_{\rm in} \gtrsim H_{\rm end}^{-3}\rho_{\rm end} \approx 1\ {\rm g}\,(10^{64}\ {\rm GeV}^4/\rho_{\rm end})^{1/2}$, while the upper bound emerges by requiring PBH evaporation before the onset of BBN: $t_{\rm ev} \simeq 1\ \sec\,(M_{\rm in}/10^8\ {\rm g})^3$. The time of evaporation $t_{\rm ev}$ can be obtained by solving the PBH mass evolution, Eq. (A1), which corresponds roughly to the condition $M_{\rm BH} = 0$ in Eq. (2), or $t_{\rm ev} \simeq \Gamma_{\rm BH}^{-1}$ when $t_{\rm in} \ll t_{\rm ev}$.

The total number of particles emitted during PBH evaporation depends on its intrinsic properties, such as the particle's spin and mass. The production rate for any species X with internal degrees of freedom g_X can be estimated as [15]

$$\frac{d\mathcal{N}_i}{dt} = \frac{27}{4}\frac{g_X\xi\zeta(3)}{16\pi^3}\frac{M_P^2}{M_{\rm BH}(t)}, \tag{7}$$

where $\xi = (1, 3/4)$ for bosonic and fermionic fields, respectively, and g_X is the internal degrees of freedom for the corresponding field. After integration we obtain,

$$\mathcal{N}_i = \frac{15 g_X\xi\zeta(3)}{g_\star(T_{\rm BH}^{\rm in})\pi^4}\begin{cases}\left(\frac{M_{\rm in}}{M_P}\right)^2, & M_X < T_{\rm BH}^{\rm in},\\ \left(\frac{M_P}{M_X}\right)^2, & M_X > T_{\rm BH}^{\rm in},\end{cases} \tag{8}$$

where M_X is the mass of the corresponding species and

$$T_{\rm BH}^{\rm in} = M_P^2/M_{\rm in} \simeq 10^{13}\left(\frac{1\ {\rm g}}{M_{\rm in}}\right)\ {\rm GeV}, \tag{9}$$

is the PBH temperature at the point of formation.[6]

Note that if one considers the production of RHNs with mass $M_N < T_{\rm BH}^{\rm in}$, PBHs should emit them from the formation time $t_{\rm in}$, whereas for $M_N > T_{\rm BH}^{\rm in}$, PBH starts to emit RHNs when PBH temperature $T_{\rm BH} \sim M_N$. Out-of-equilibrium production of RHNs is a key ingredient in the leptogenesis scenario. Indeed, SM can be extended by taking three right-handed SM singlet massive neutrino N_i ($i = 1, 2, 3$) with the interaction Lagrangian,

$$\mathcal{L} \supset -\frac{1}{2}\sum_i M_{N_i}\overline{N_i^c}N_i - y_N^{ij}\overline{N_i}\tilde{H}^\dagger L_j + {\rm H.c.}, \tag{10}$$

where SM left-handed leptons doublets are identified as L_i and $\tilde{H} = i\sigma_2 H^*$ where H represents the SM Higgs doublet. $\sigma_{\rm i}$ are the Pauli spin matrices. We detail the Yukawa coupling parametrization in the Appendix B. We assume the Majorana masses M_{N_i} to be hierarchical $M_{N_1} \ll M_{N_{2,3}}$. Moreover, for the decay of heavier RHNs $N_{2,3}$, we consider lepton-number-violating interactions of N_1 rapid enough to wash out the lepton-number asymmetry originated by the other two. Therefore, only the CP-violating asymmetry from the decay of N_1 survives and is relevant for leptogenesis.[7]

Once right-handed neutrinos are produced from the evaporating PBHs, they can decay later and produce lepton asymmetry, which can be converted into the baryon asymmetry through the Standard Model electroweak sphaleron process. At the origin of the asymmetry generation, right-handed neutrino decay rapidly into left-handed lepton L and Higgs doublets H, $N \to L + H$, and $N \to \overline{L} + \tilde{H}$ and if CP is violated, the lepton asymmetry is then given by

$$Y_L = \frac{n_L}{s} = \kappa_{\Delta L}\frac{n_{N_1}}{s}, \tag{11}$$

where $s = \frac{2\pi^2}{45}g_*(T)T^3$ represents entropy energy density with radiation temperature T, and the CP asymmetry generated from N_1 decay is given by [61]

$$\kappa_{\Delta L} \equiv \frac{\Gamma_{N_1\to\ell_i H} - \Gamma_{N_1\to\overline{\ell}_i\tilde{H}}}{\Gamma_{N_1\to\ell_i H} + \Gamma_{N_1\to\overline{\ell}_i\tilde{H}}}$$
$$\simeq \frac{1}{8\pi}\frac{1}{(y_N^\dagger y_N)_{11}}\sum_{j=2,3}{\rm Im}(y_N^\dagger y_N)_{1j}^2 \times \mathcal{F}\left(\frac{M_{N_j}^2}{M_{N_1}^2}\right), \tag{12}$$

with

$$\mathcal{F}(x) \equiv \sqrt{x}\left[\frac{1}{1-x} + 1 - (1+x)\log\left(\frac{1+x}{x}\right)\right]. \tag{13}$$

This can be further simplified to [77,111]

[5] A more comprehensive expression for greybody factor can be found, for example, in Refs. [23,29,110].

[6] For the mass scale we consider in the work, $g_\star = 106.75$, $T_{\rm BH}$ being much larger than the electroweak scale, all the SM degrees of freedom should be taken into account.

[7] The effects due to $N_{2,3}$ can be neglected as long as $\max[T_{\rm RH}, T_{\rm ev}] < M_{N_{2,3}}$, which we consider in the present analysis. In the opposite case, L-violating interactions of N_1 does not wash out any lepton asymmetry generated at temperatures $T \gg M_{N_1}$ via decays of $N_{2,3}$. In such scenarios, the lepton asymmetry generated in $N_{2,3}$ decays survives the N_1 leptogenesis phase.

$$|\kappa_{\Delta L}| \simeq \frac{3\delta_{\rm eff}}{16\pi}\frac{M_{N_1} m_{\nu_i}}{v^2} \simeq 10^{-6}\delta_{\rm eff}\left(\frac{M_{N_1}}{10^{10}}\right)\left(\frac{m_{\nu_i}}{0.05\ {\rm eV}}\right), \quad (14)$$

where $i = 2, 3$ for normal hierarchy and $\delta_{\rm eff}$ is the effective CP-violating phase (see Appendix C for details)

$$\delta_{\rm eff} = \frac{1}{(y_N)_{13}^2}\frac{{\rm Im}(y_N^\dagger y_N)_{13}^2}{(y_N^\dagger y_N)_{11}}, \quad (15)$$

whereas $v = 174$ GeV is the Higgs vacuum expectation value. Note that a similar CP-asymmetry parameter can be obtained for the inverted hierarchy with $i = 1, 2$. We consider m_{ν_3} to be the heaviest active neutrino mass. The produced lepton asymmetry is eventually converted to baryon asymmetry via electroweak sphaleron processes, leading to baryon number yield at the point of evaporation [37,39,43],

$$Y_B(a_{\rm ev}) = \frac{n_B}{s}\bigg|_{a_{\rm ev}} = \mathcal{N}_{N_1}\kappa_{\Delta L} a_{\rm sph}\frac{n_{\rm BH}(a_{\rm ev})}{s(a_{\rm ev})}, \quad (16)$$

where $a_{\rm sph} = \frac{28}{79}$ and $n_{\rm BH}(a_{\rm ev})$ is the PBH number density at the end of the evaporation process when the scale factor is $a_{\rm ev}$.

B. Leptogenesis during PBH reheating

In the PBH reheating scenario, the decay of PBHs is sufficient to reheat the Universe [58]. If we assume no further entropy production after PBH evaporation, the asymmetry is conserved and is given by $Y_B^0 = Y_B(a_{\rm ev})$. However, depending on the initial population density, PBH reheating can be accomplished in two ways. If we define

$$\beta = \frac{\rho_{\rm BH}}{\rho_{\rm tot}}\bigg|_{\rm in}, \quad (17)$$

as the ratio between PBH energy density and the background energy density at the point of formation, it was shown in [58,59] that in the presence of inflaton field ϕ, for β larger than some critical value $\beta_{\rm c}$ given by

$$\beta_c = \left[\frac{\epsilon}{2\pi\gamma(1+w_\phi)}\right]^{\frac{2w_\phi}{1+w_\phi}}\left(\frac{M_P}{M_{\rm in}}\right)^{\frac{4w_\phi}{1+w_\phi}} \simeq (7.6\times10^{-6})^{\frac{4w_\phi}{1+w_\phi}}\left(\frac{1\ {\rm g}}{M_{\rm in}}\right)^{\frac{4w_\phi}{1+w_\phi}}, \quad (18)$$

where $w_\phi = (n-2)/(n+2)$ is the equation of state of an inflaton oscillating in a potential $V(\phi) \propto \phi^n$ (see Appendix D for details), PBH energy density dominates over that of inflaton before the evaporation process is complete. From Eq. (18), we find, $\beta_c \simeq 7.6\times10^{-6}(\frac{1\ {\rm g}}{M_{\rm in}})$ for $n = 4$, and $\beta_c \simeq 9.3\times10^{-8}(\frac{1\ {\rm g}}{M_{\rm in}})^{\frac{4}{3}}$ for $n = 6$. We show in Fig. 1 the variation of β_c with $M_{\rm in}$ for different choices of n.

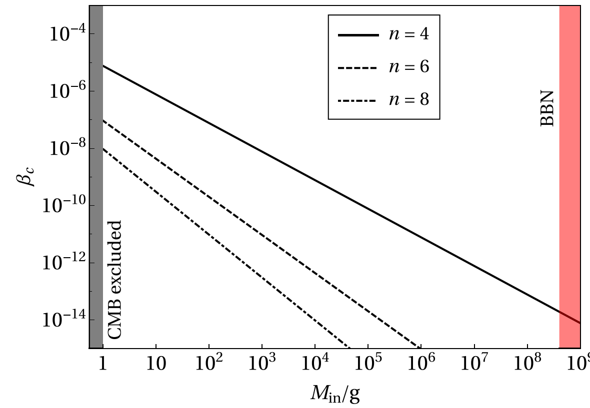

FIG. 1. β_c as a function of $M_{\rm in}$ for different choices of n, following Eq. (18), where the shaded regions are discarded from CMB bound on the inflationary Hubble scale (in gray) and BBN bound (in red).

On the other hand, if $\beta < \beta_{\rm c}$, even if the reheating is mainly generated by the PBHs, the entire PBH evanescence takes place in an inflaton-dominated background. Indeed, reheating can still be achieved through evaporating PBHs if the inflaton coupling is small enough and less than some critical value $y_\phi^{\rm c}$ (see Appendix D). Additionally, it is also required that the inflaton energy density redshifts faster than the radiation energy density, i.e., $w_\phi > 1/3$ (or $n > 4$). This distinction between a PBH evaporation during (or not) the inflaton domination era is crucial for the dilution of the different densities, and therefore for the baryonic asymmetry $Y_B(a_{\rm ev})$.

1. Scenario-I: $\beta > \beta_{\rm c}$

Solving the Boltzmann equation, we find for the evolution of inflaton density [112,113],

$$\rho_\phi = \rho_{\rm end}\left(\frac{a_{\rm end}}{a}\right)^{3(1+w_\phi)} = \rho_{\rm end}\left(\frac{a_{\rm end}}{a}\right)^{\frac{6n}{n+2}}, \quad (19)$$

whereas

$$\rho_{\rm BH} = n_{\rm BH}M_{\rm BH} \propto a^{-3}. \quad (20)$$

This means that for $n > 2$ and sufficiently long-lived PBH, the PBH can dominate the energy budget of the Universe at a time $t_{\rm BH}$ corresponding to the scale factor $a_{\rm BH}$, before they evaporate. Since PBHs are formed during inflaton domination while they evaporate during PBH domination, from Eq. (2), the PBH mass evolves as

$$M_{\rm BH}^3 \simeq M_{\rm in}^3 - \frac{2\sqrt{3}\epsilon M_P^5}{\sqrt{\rho_\phi(a_{\rm BH})}}\left(\frac{a}{a_{\rm BH}}\right)^{3/2}, \quad (21)$$

where we assume $a_{\rm ev} \gg a_{\rm BH}$ for which $M_{\rm BH}(a_{\rm BH}) \simeq M_{\rm in}$. We then obtain the scale factor associated with the evaporation time [58]

$$\frac{a_{\rm ev}}{a_{\rm BH}} = \frac{M_{\rm in}^2 \rho_{\rm end}^{\frac{1}{3}}}{(2\sqrt{3}\epsilon M_P^5)^{\frac{2}{3}}} \left(\frac{a_{\rm end}}{a_{\rm BH}}\right)^{(1+w)}, \tag{22}$$

imposing the condition $M(a_{\rm ev}) = 0$, where $a_{\rm BH}$ corresponds to the onset of PBH domination [58]

$$\frac{a_{\rm BH}}{a_{\rm end}} = \left(\frac{M_{\rm in} H_{\rm end}}{4\pi\gamma M_P^2}\right)^{\frac{2}{3(1+w_\phi)}} \beta^{-\frac{1}{3w_\phi}}. \tag{23}$$

We will be exploiting these relations in Sec. III and Sec. IV.

For $\beta > \beta_{\rm c}$ evaporation is completed during PBH domination; hence, reheating and evaporation points are identical, i.e., $T(a_{\rm ev}) \equiv T_{\rm RH}$. Since PBH domination behaves like a dustlike equation of state ($w_{\rm BH} = 0$), the Hubble parameter at the time of evaporation reads,

$$H(a_{\rm ev}) = \frac{2}{3t_{\rm ev}} = \frac{2\Gamma_{\rm BH}}{3}. \tag{24}$$

Utilizing this expression, one can find the reheating temperature,

$$\frac{\rho_{\rm RH}}{3M_P^2} = H^2(a_{\rm ev}) \Rightarrow T_{\rm RH} = \left(\frac{12\epsilon^2}{\alpha_T}\right)^{\frac{1}{4}} M_P \left(\frac{M_P}{M_{\rm in}}\right)^{\frac{3}{2}}, \tag{25}$$

where $\alpha_T = \frac{\pi^2}{30} g_{\rm RH}$, and $g_{\rm RH} = 106.75$ is the degrees of freedom associated with the thermal bath at $T_{\rm RH}$.

To determine the RHN yield at the point of evaporation, one needs to compute BH number density at $a_{\rm ev}$, which reads,

$$n_{\rm BH}(a_{\rm ev}) \simeq \frac{\rho_{\rm BH}(a_{\rm ev})}{M_{\rm in}} = \frac{\rho_{\rm RH}}{M_{\rm in}} = \frac{12\epsilon^2 M_P^{10}}{M_{\rm in}^7}. \tag{26}$$

Equation (26), together with Eq. (25) provides

$$\frac{n_{\rm BH}(a_{\rm ev})}{T^3(a_{\rm ev})} = (12\epsilon^2\alpha_T^3)^{\frac{1}{4}} \left(\frac{M_P}{M_{\rm in}}\right)^{\frac{5}{2}} \simeq 4\times 10^{-12} \left(\frac{1\ {\rm g}}{M_{\rm in}}\right)^{\frac{5}{2}}. \tag{27}$$

One can then compute the final baryon asymmetry utilizing Eq. (16)

$$Y_B(T_0) \simeq 8.7\times 10^{-11} \delta_{\rm eff} \left(\frac{m_{\nu,\rm max}}{0.05\ {\rm eV}}\right) \times \begin{cases} \left(\frac{M_{N_1}}{3.7\times 10^{11}\ {\rm GeV}}\right) \times \left(\frac{1\ {\rm g}}{M_{\rm in}}\right)^{\frac{1}{2}}, & M_{N_1} < T_{\rm BH}^{\rm in} \\ \left(\frac{3\times 10^{14}\ {\rm GeV}}{M_{N_1}}\right) \times \left(\frac{1\ {\rm g}}{M_{\rm in}}\right)^{\frac{5}{2}}, & M_{N_1} > T_{\rm BH}^{\rm in}, \end{cases} \tag{28}$$

where $g_j = 2$ for Majorana-like RHNs is considered. The interesting point is that, for a given PBH mass, considering $\delta_{\rm eff} \lesssim \mathcal{O}(1)$, two regions are allowed for M_{N_1}.

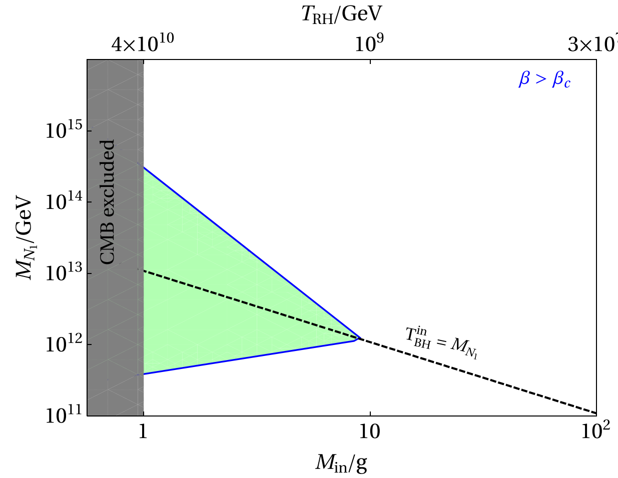

FIG. 2. Viable parameter space in the $[M_{N_1}, M_{\rm in}]$ plane, considering $\beta > \beta_c$. For each $M_{\rm in}$ corresponding $T_{\rm RH}(T_{\rm ev})$ is mentioned along the top axis. The gray shaded region is disallowed from CMB bound on the scale of inflation for $n = 6$ [cf. Eq. (1)].

In Fig. 2, we show in green the allowed region of the parameter space ($M_{\rm in}$, M_{N_1}) that can satisfy the observed baryon asymmetry for $\beta > \beta_c$. The slope of the two boundaries (in blue) is dictated by Eq. (28) setting $\delta_{\rm eff} = 1$. We recognize the limit $M_{N_1} \propto M_{\rm in}^{1/2}$ for $M_{N_1} < T_{\rm BH}^{\rm in}$, while for $M_{N_1} > T_{\rm BH}^{\rm in}$, $M_{N_1} \propto M_{\rm in}^{-5/2}$. Within the green shaded region, surrounded by the two boundaries, depending on the choice of $\delta_{\rm eff}$, it is possible to achieve the observed baryon asymmetry for a given M_{N_1}. The lower bound on PBH mass obtained from the gray-shaded region is set by the maximum energy scale of inflation, which is constrained by the CMB observation. It is important to note here that the allowed region also satisfies the hierarchy $M_{N_1} > T(a_{\rm ev}) \equiv T_{\rm RH}$, validating nonthermal leptogenesis. Otherwise, for $M_{N_1} < T(a_{\rm ev})$, the RHNs produced from PBH evaporation are in the thermal bath, and washout processes can not be neglected [39]. Thus, our first result is that for $\beta > \beta_c$, the right baryon asymmetry is achievable for $10^{12} \lesssim M_{N_1} \lesssim 10^{15}$ GeV and PBH mass $M_{\rm in} \lesssim \mathcal{O}(10)$ g. Heavier PBH masses do not have a sufficient number density to produce RHN in the right amount to fit with the measured $Y_B(T_0)$ as it is clear from Eq. (28).

2. Scenario-II: $\beta < \beta_c$

For $\beta < \beta_{\rm c}$, PBHs are formed *and* evaporate during inflaton domination. In contrast to the previous case, PBHs never dominate the entire energy component of the Universe. Indeed, if the inflaton-matter coupling strength is less than some critical value y_ϕ^c given in the Appendix, see Eq. (D13), and the inflaton equation of state mimics that of a stiff fluid, $w_\phi > 1/3$, there is a possibility for the PBHs to be responsible of the reheating even if not dominating the energy budget [58]. Another way of looking at things is to note that for a given Yuwaka coupling y_ϕ, there always exists a threshold value of β, namely, $\beta_{\rm BH}$, above which PBH evaporation governs reheating temperature (see Appendix D for details). One can find the expression for $\beta_{\rm BH}$ for an inflaton potential $V(\phi) = \lambda M_P^4 (\frac{\phi}{M_P})^n$ as [58]

$$\beta_{\rm BH} = \left(\frac{y_\phi \alpha_n}{8\pi}\right)^{\frac{2(3w_\phi - 1)}{3(1-w_\phi)}} \left(\frac{48\pi^2}{\lambda}\right)^{\frac{1-3w_\phi}{3(1+w_\phi)}} \times \left(\frac{\epsilon \gamma^{-3w_\phi}}{2\pi(1+w_\phi)}\right)^{\frac{2}{3(1+w_\phi)}} \left(\frac{M_P}{M_{\rm in}}\right)^{\frac{2(1-w_\phi)}{(1+w_\phi)}}, \quad (29)$$

where $\bar{\alpha}_n = \frac{2(1+w_\phi)}{(5-9w_\phi)} \sqrt{\frac{6(1+w_\phi)(1+3w_\phi)}{(1-w_\phi)^2}}$. The above equation is true for $n < 7$, whereas for $n > 7$, we have

$$\beta_{\rm BH} = -\frac{y_\phi^2 \alpha_n}{8\pi} (48\pi^2)^{\frac{1-3w_\phi}{3(1+w_\phi)}} \lambda^{\frac{1-w_\phi}{2(1+w_\phi)}} \left(\frac{\epsilon \gamma^{-3w_\phi}}{2\pi(1+w_\phi)}\right)^{\frac{2}{3(1+w_\phi)}} \times \left(\frac{M_P}{M_{\rm in}}\right)^{\frac{2(1-w_\phi)}{1+w_\phi}} \left(\frac{\rho_{\rm end}}{M_P^4}\right)^{\frac{9w_\phi - 5}{6(1+w_\phi)}}. \quad (30)$$

In this case, considering that after evaporation, all the PBH energy density is converted into the radiation energy density, $\rho_{\rm BH}(a_{\rm ev}) \simeq \rho_{\rm R}(a_{\rm ev}) = \alpha_T T_{\rm ev}^4$, we obtain

$$\frac{n_{\rm BH}(a_{\rm ev})}{T_{\rm ev}^3} \simeq \left(\frac{\alpha_T^3 \rho_{\rm BH}(a_{\rm ev})}{M_{\rm in}^4}\right)^{\frac{1}{4}}. \quad (31)$$

Since the PBHs behave like matter,

$$\rho_{\rm BH}(a_{\rm ev}) = \beta \rho_\phi(a_{\rm in}) \left(\frac{a_{\rm in}}{a_{\rm ev}}\right)^3 = 48\pi^2 \gamma^2 \beta \frac{M_P^6}{M_{\rm in}^2} \left(\frac{a_{\rm in}}{a_{\rm ev}}\right)^3, \quad (32)$$

where we used from Eq. (1)

$$\rho_\phi(a_{\rm in}) = 48\pi^2 \gamma^2 \frac{M_P^6}{M_{\rm in}^2}. \quad (33)$$

Considering that PBHs formed and evaporate during inflaton domination, we obtain

$$\left(\frac{a_{\rm in}}{a_{\rm ev}}\right)^3 = \left(\frac{H_{\rm ev}}{H_{\rm in}}\right)^{\frac{2}{1+w_\phi}} = \left(\frac{\epsilon}{2(1+w_\phi)\pi\gamma} \frac{M_P^2}{M_{\rm in}^2}\right)^{\frac{2}{1+w_\phi}}, \quad (34)$$

where we used $H_{\rm in}$ given by Eq. (1) and the Hubble parameter at evaporation,

$$H_{\rm ev} = H(a_{\rm ev}) = \frac{2}{3(1+w_\phi)} \frac{1}{t_{\rm ev}} = \frac{2}{3(1+w_\phi)} \Gamma_{\rm BH}. \quad (35)$$

Combining Eqs. (32) and (34), we can compute the PBH energy density at evaporation time,

$$\rho_{\rm BH}(a_{\rm ev}) = 48\pi^2 \beta \left(\frac{\gamma^{w_\phi} \times \epsilon}{2\pi(1+w_\phi)}\right)^{\frac{2}{1+w_\phi}} M_P^4 \left(\frac{M_P}{M_{\rm in}}\right)^{\frac{6+2w_\phi}{1+w_\phi}}. \quad (36)$$

Substituting the above expression into Eq. (31), we find

$$\frac{n_{\rm BH}(a_{\rm ev})}{T_{\rm ev}^3} = (48\pi^2 \beta \alpha_T^3)^{\frac{1}{4}} \mu \left(\frac{M_P}{M_{\rm in}}\right)^{\frac{5+3w_\phi}{2(1+w_\phi)}}, \quad (37)$$

where $\mu = (\frac{\gamma^{w_\phi} \epsilon}{2\pi(1+w_\phi)})^{\frac{1}{2(1+w_\phi)}}$. Finally, using Eq. (16), we obtain

$$Y_B(T_0) \simeq 8.7 \times 10^{-11} \delta_{\rm eff} \left(\frac{m_{\nu,\rm max}}{0.05 \text{ eV}}\right) \mu \beta^{\frac{1}{4}} \times \begin{cases} \left(\frac{M_{N_1}}{6.5\times 10^8 \text{ GeV}}\right) \times \left(\frac{M_P}{M_{\rm in}}\right)^{\frac{1-w_\phi}{2(1+w_\phi)}}, & M_{N_1} < T_{\rm BH}^{\rm in} \\ 7 \times 10^{18} \left(\frac{6.5\times 10^8 \text{ GeV}}{M_{N_1}}\right) \times \left(\frac{M_P}{M_{\rm in}}\right)^{\frac{5+3w_\phi}{2(1+w_\phi)}}, & M_{N_1} > T_{\rm BH}^{\rm in}, \end{cases} \quad (38)$$

One important point is to note that, in contrast with the previous case, here, final asymmetry strictly depends on the β value as well as the background equation of the state where PBHs are formed and evaporated. Whereas, for $\beta > \beta_{\rm c}$ case, baryon asymmetry only depends on the formation mass $M_{\rm in}$, and does not depend on the equation of state of the background.

The viable parameter space corresponding to $\beta < \beta_c$ is shown in Fig. 3, where, as before, the maximally allowed region satisfying the observed baryon asymmetry is shown in the $(M_{\rm in}, M_{N_1})$ plane for $\beta = 10^{-10}$ and different values of n (left), and for $n = 6$ and different values of β (right). As in Fig. 2, the green shaded region represents the parameter space where the right baryonic asymmetry can be obtained by tuning $\delta_{\rm eff}$ accordingly. As expected, as the density of PBH is lower than the previous case ($\beta < \beta_c$), it is more difficult to generate a reasonable asymmetry Y_B. This results in a more restricted parameter space. In the left panel, we see, a smaller equation of state (smaller n) restricts even more the parameter space for a given $\beta = 10^{-10}$. Note that the slopes of the boundaries ($\delta_{\rm eff} = 1$) follow Eq. (38), where, for $n = 6$, $M_{N_1} \propto M_{\rm in}^{1/6}$ when $M_{N_1} < T_{\rm BH}^{\rm in}$ and $M_{N_1} \propto M_{\rm in}^{-13/6}$ for $M_{N_1} > T_{\rm BH}^{\rm in}$. For $n = 8$, we find $M_{N_1} \propto M_{\rm in}^{1/8}$ for $M_{N_1} < T_{\rm BH}^{\rm in}$, and $M_{N_1} \propto M_{\rm in}^{-17/8}$ in the other case. This comes from the fact that the inflaton field redshifted faster for a stiffer background (larger n). Consequently, the relative density increment of PBHs is larger, which makes it easier to generate correct baryon asymmetry. As a result, in order to obtain the right baryon asymmetry in a stiffer background, the RHN is required to be lighter for $M_{N_1} < T_{\rm BH}^{\rm in}$, while for $M_{N_1} > T_{\rm BH}^{\rm in}$, heavier RHN is needed since for a fixed $M_{\rm in}$ we see

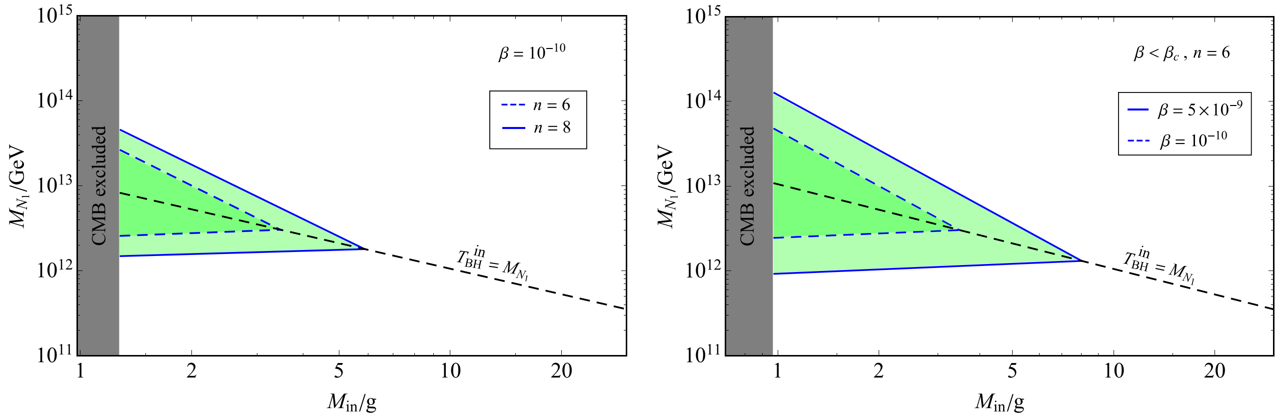

FIG. 3. Left: Allowed parameter space for $\beta = 10^{-10} < \beta_c$, considering two different background equation of states, shown via different shades. Right: Same as left, but for a fixed $n = 6$, considering two different β values. In both plots, the gray shaded region is disallowed from CMB constraint on the scale of inflation [cf. Eq. (1)].

$$Y_B^0 \propto \frac{n_{\rm BH}}{T^3}\bigg|_{\rm ev} \times \frac{M_{N_1} m_{\nu,\rm max}}{v^2} \begin{cases} \left(\frac{M_{\rm in}}{M_P}\right)^2, & M_{N_1} < T_{\rm BH}^{\rm in} \\ \left(\frac{M_P}{M_{N_1}}\right)^2, & M_{N_1} < T_{\rm BH}^{\rm in}. \end{cases} \tag{39}$$

On the other hand, as expected and clear from Eq. (38), larger values of β enlarge the possibility of obtaining the right Y_B. In the right panel of Fig. 3, we show the allowed parameter space with two different values of $\beta = \{5 \times 10^{-9}, 10^{-10}\}$, for a fixed $n = 6$. The PBH yields at $a_{\rm ev}$ increases monotonically with β, see Eq. (37), hence, for a fixed $M_{\rm in}$, a larger β results in comparatively larger viable parameter space.

At this stage of our study, a preliminary conclusion would be that the necessary PBHs mass, which allows for a viable baryogenesis through their decay while still ensuring the reheating, is $M_{\rm in} \lesssim 10$ g. Heavier PBHs are not sufficiently dense to generate the observed Y_B asymmetry. When the background is dominated by the inflaton field, the parameter space is even reduced due to a dilution affecting the PBH. We can now see how the parameter space can evolve if the reheating is led by the inflaton decay.

C. Leptogenesis during inflaton reheating

We now analyze the scenario where the direct decay of inflaton takes the leading role in completing the reheating. We consider a minimal reheating process through the Yukawa interaction $y_\phi \phi \bar{f} f$ between the inflaton and the SM-like fermion fields.[8] For $\beta < \beta_c$, one can obtain a critical value of the Yukawa coupling strength y_ϕ^c, such that for $y_\phi > y_\phi^c$ the reheating is always determined by the inflaton decay (see Appendix D for details). In this case, the parameter space will be even reduced, compared to the previous situations, due to the dilution effect between the evaporation end (when PBH decays) and the end of reheating (when the inflaton decays).

Indeed, if reheating occurs after PBH evaporation, then due to entropy injection between $a_{\rm ev} < a < a_{\rm RH}$, the final asymmetry reads,

$$Y_B(T_0) = Y_B(T_{\rm RH}) = \mathcal{N}_{N_1} \epsilon_{\Delta L} a_{\rm sph} \frac{n_{\rm BH}(a_{\rm ev})}{s(a_{\rm RH})} \left(\frac{a_{\rm ev}}{a_{\rm RH}}\right)^3. \tag{40}$$

Connecting the scale factor from the point of evaporation to the end of reheating, one can find

$$\frac{a_{\rm ev}}{a_{\rm RH}} = \left(\frac{t_{\rm ev}}{t_{\rm RH}}\right)^{\frac{2}{3(1+w_\phi)}} = \left[\frac{3(1+w_\phi)}{2}\frac{H_{\rm RH}}{\Gamma_{\rm BH}}\right]^{\frac{2}{3(1+w_\phi)}} = \left(\frac{(1+w_\phi)}{2\sqrt{3}}\frac{\sqrt{\alpha_T}T_{\rm RH}^2}{M_P}\frac{M_{\rm in}^3}{\epsilon M_P^4}\right)^{\frac{2}{3(1+w_\phi)}}, \tag{41}$$

where $H_{\rm RH}$ denotes the Hubble parameter at the end of reheating. Thus, the RHN number density at the end of reheating reads,

$$\frac{n_N(a_{\rm RH})}{T_{\rm RH}^3} = \mathcal{C}\begin{cases} \left(\frac{M_P}{T_{\rm RH}}\right)^{\frac{3w_\phi-1}{1+w_\phi}}\left(\frac{M_{\rm in}}{M_P}\right)^{\frac{1-w_\phi}{1+w_\phi}}, & M_{N_1} < T_{\rm BH}^{\rm in} \\ \frac{M_P^2}{M_{N_1}^2}\left(\frac{M_P}{T_{\rm RH}}\right)^{\frac{3w_\phi-1}{1+w_\phi}}\left(\frac{M_P}{M_{\rm in}}\right)^{\frac{1+3w_\phi}{1+w_\phi}}, & M_{N_1} > T_{\rm BH}^{\rm in} \end{cases} \tag{42}$$

where $\mathcal{C} = \tilde{\mu}\frac{540 g_j \zeta(3)\beta}{g_*(T_{\rm BH})\pi^2}$, with $\tilde{\mu} = \left(\frac{\sqrt{\alpha_T}\gamma^{w_\phi}}{4\sqrt{3}\pi}\right)^{\frac{2}{1+w_\phi}}$. The final baryon asymmetry thus reads,

[8] It is worth noting that such an interaction can lead to fermion preheating [114], for which the production of particles is resonantly suppressed, a consequence of Fermi-Dirac statistics.

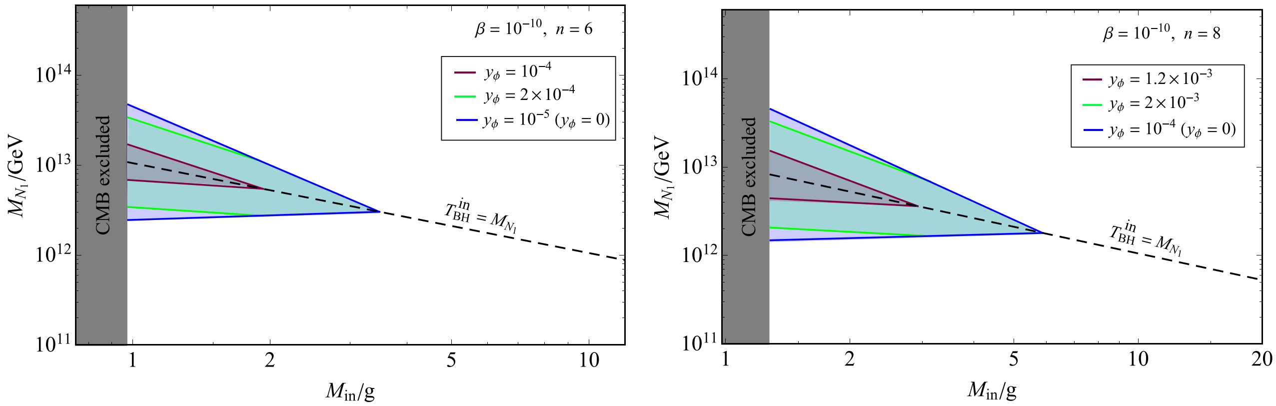

FIG. 4. Left: Parameter space showing observed baryon asymmetry for a fixed value of $n = 6$, and three different choices of the Yukawa coupling y_ϕ, shown via different shades. Right: Same as left, but for $n = 8$. In both plots, the gray-shaded region is disallowed from CMB constraint on the scale of inflation [cf. Eq. (1)]. For coupling strengths less than the critical value y_ϕ^c [cf. Eq. (D13)], below which PBH evaporation leads the reheating, behaves similarly as $y_\phi = 0$.

$$Y_B(T_0) \simeq 8.7\times10^{-11}\delta_{\rm eff}\left(\frac{m_{\nu,\rm max}}{0.05\ {\rm eV}}\right)\left(\frac{M_P}{T_{\rm RH}}\right)^{\frac{3w_\phi-1}{1+w_\phi}}\tilde{\mu}\beta \times\begin{cases}\left(\frac{M_{N_1}}{9.5\times10^7\ {\rm GeV}}\right)\times\left(\frac{M_{\rm in}}{M_P}\right)^{\frac{1-w_\phi}{1+w_\phi}}, & M_{N_1} < T_{\rm BH}^{\rm in}\\ 6.2\times10^{13}\left(\frac{10^{15}\ {\rm GeV}}{M_{N_1}}\right)\times\left(\frac{M_P}{M_{\rm in}}\right)^{\frac{1+3w_\phi}{1+w_\phi}}, & M_{N_1} > T_{\rm BH}^{\rm in}.\end{cases} \tag{43}$$

Note that, in the present framework, we are always interested in the case where PBHs are formed during the reheating, implying $a_{\rm in} < a_{\rm RH}$. They can evaporate before ($a_{\rm ev} < a_{\rm RH}$) or after ($a_{\rm ev} > a_{\rm RH}$) the end of reheating, it was shown in Refs. [58,59], that both cases lead to the same result. This can be understood from the following argument. At the present epoch, the number density of any particle j, produced via PBH evaporation is given by

$$n_j(a_0) = n_j(a_{\rm ev})\left(\frac{a_{\rm ev}}{a_0}\right)^3 = n_{\rm BH}(a_{\rm ev})\mathcal{N}_j\left(\frac{a_{\rm ev}}{a_0}\right)^3,$$

where $n_j(a_{\rm ev})$ and $n_{\rm BH}(a_{\rm ev})$ are the particle and PBH number density at the point of evaporation. This can be further written as

$$n_j(a_0) = n_{\rm BH}(a_{\rm in})\mathcal{N}_j\left(\frac{a_{\rm in}}{a_0}\right)^3 = n_{\rm BH}(a_{\rm in})\mathcal{N}_j\left(\frac{a_{\rm in}}{a_{\rm RH}}\right)^3\left(\frac{a_{\rm RH}}{a_0}\right)^3. \tag{44}$$

If the dilution is dominated by the same field (in this case, the inflaton) between $a_{\rm in}$ and $a_{\rm RH}$, the relic abundance does not depend on the epoch of evaporation. Thus, irrespective of $a_{\rm ev} < a_{\rm RH}$ or $a_{\rm ev} > a_{\rm RH}$, the final result shall remain unaffected.

We show in Fig. 4 the effect of inflaton reheating on the parameter space producing right baryon asymmetry in the $(M_{\rm in}, M_{N_1})$ plane for fixed choices of β and y_ϕ, for $n = 6$ (left) and $n = 8$ (right). As expected, larger values of y_ϕ constrains even more the allowed parameter space. Indeed, a stronger coupling results in higher $T_{\rm RH}$ due to the earlier decay of the inflaton, when it stores a larger amount of energy. This earlier decay tends to dilute even further the baryon asymmetry generated by the PBH decay. As a result, the right abundance is obtained with heavier RHNs for $M_{N_1} < T_{\rm BH}^{\rm in}$, and the opposite for $M_{N_1} > T_{\rm BH}^{\rm in}$. Increasing n dilutes slightly more the inflaton before its decay, lowering $T_{\rm RH}$ and reopening very little parameter space, as one can see in the right panel of Fig. 4 for $n = 8$. It is interesting to note that since for $y_\phi < y_\phi^c$, PBH decay dominates over inflaton decay, hence all such couplings can effectively treated to be zero. This happens, for example,

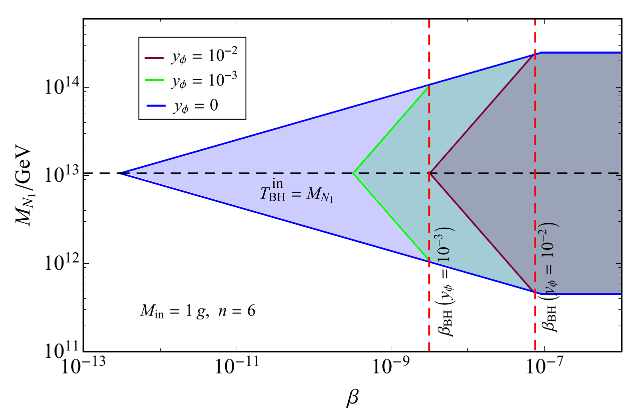

FIG. 5. Parameter space for right baryon asymmetry for a fixed BH mass $M_{\rm in} = 1$ g and $n = 6$, considering different choices of y_ϕ, as shown via different shades. The red dashed line represents the threshold values of β, $\beta_{\rm BH}$ [cf. Eq. (29)] above which evaporating PBHs always dominate the reheating process.

with $y_\phi = 10^{-5}$ for $n = 6$ and $\beta = 10^{-10}$ as mentioned in the left panel of Fig. 4.

In Fig. 5, we show the viable parameter space for different choices of y_ϕ while fixing $M_{\rm in} = 1$ g and $n = 6$. To the left of each vertical red dashed line, the Universe is reheated via inflaton. To the right we see, $M_{N_1} \propto \beta^{-1}$ for $M_{N_1} < T_{\rm BH}^{\rm in}$ and $M_{N_1} \propto \beta$ for $M_{N_1} > T_{\rm BH}^{\rm in}$, following Eq. (43). Once $\beta > \beta_c$, the abundance depends only on the PBH lifetime and becomes independent of β. In conclusion, we showed that if one wants to reconcile a viable baryonic asymmetry generated by PBH decay, the mass spectrum should lie in a region $M_{\rm BH} \lesssim 10$ g, whatever the reheating process. However, another minimal gravitational source of baryonic asymmetry exists, which is through the exchange of a graviton.

III. MINIMAL GRAVITATIONAL LEPTOGENESIS IN THE PRESENCE OF PBH

Another gravitationally sourced asymmetry involves the scattering of the inflaton during reheating, that leads to the production of the heavy RHNs through the exchange of a graviton, depicted in Fig. 6. This was studied in [77,78] and is considered as a minimal, unavoidable source of leptogenesis. In this section, we will not suppose any coupling between the inflaton and the SM, except for the gravitational one ($y_\phi = 0$).

Gravitational production can be achieved by considering the following interaction Lagrangian:

$$\sqrt{-g}\mathcal{L}_{\rm int} = -\frac{1}{M_P} h_{\mu\nu}(T^{\mu\nu}_{\rm SM} + T^{\mu\nu}_{\phi} + T^{\mu\nu}_{X}), \qquad (45)$$

where X is a particle that does not belong to the SM, which is a spin $1/2$ Majorana fermion in the present context. The gravitational field can be realized by expanding the metric around Minkowski space-time $\eta_{\mu\nu}$ as $g_{\mu\nu} \simeq \eta_{\mu\nu} + \frac{2h_{\mu\nu}}{M_P}$, where $h_{\mu\nu}$ represents the canonically normalized quanta of the graviton. The graviton propagator for momentum p is

$$\Pi^{\mu\nu\rho\sigma}(p) = \frac{\eta^{\rho\nu}\eta^{\sigma\mu} + \eta^{\rho\mu}\eta^{\sigma\nu} - \eta^{\rho\sigma}\eta^{\mu\nu}}{2p^2}. \qquad (46)$$

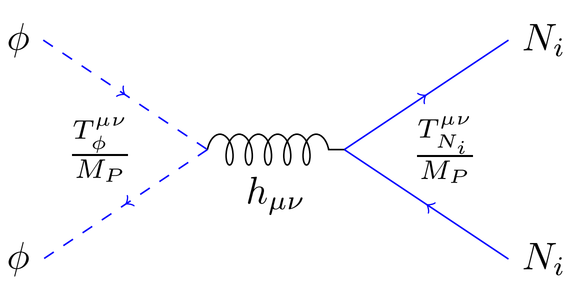

FIG. 6. Production of RHNs N_i mediated by gravity during reheating, where $T^{\mu\nu}$ represents corresponding energy-momentum tensor.

The form of the stress-energy tensor $T_i^{\mu\nu}$ depends on the spin of the field and for Majorana spin-$1/2$ fermions χ, takes the form,

$$T^{\mu\nu}_{1/2} = \frac{i}{8}[\bar{\chi}\gamma^\mu \overleftrightarrow{\partial}^\nu \chi + \bar{\chi}\gamma^\nu \overleftrightarrow{\partial}^\mu \chi] - g^{\mu\nu}\left[\frac{i}{4}\bar{\chi}\gamma^\alpha \overleftrightarrow{\partial}_\alpha \chi - \frac{m_\chi}{2}\overline{\chi^c}\chi\right], \qquad (47)$$

whereas for a generic scalar S,

$$T^{\mu\nu}_0 = \partial^\mu S \partial^\nu S - g^{\mu\nu}\left[\frac{1}{2}\partial^\alpha S \partial_\alpha S - V(S)\right]. \qquad (48)$$

As before, the heavy RHNs undergo CP-violating decay to produce the lepton asymmetry. Since we are considering nonthermal leptogenesis, hence we only take inflaton scatterings into account.[9]

For the production of N_1 through the scattering of the inflaton condensate, we consider the time-dependent oscillations of a classical inflaton field $\phi(t)$. The oscillating inflaton field with a time-dependent amplitude can be parametrized as

$$\phi(t) = \phi_0(t) \cdot \mathcal{Q}(t) = \phi_0(t) \sum_{\nu=-\infty}^{\infty} \mathcal{Q}_n e^{-i\nu\omega t}, \qquad (49)$$

where $\phi_0(t)$ is the time-dependent amplitude that includes the effects of redshift and $\mathcal{Q}(t) = \sum_{\nu=-\infty}^{\infty} \mathcal{Q}_n e^{-i\nu\omega t}$ describes the periodicity of the oscillation of the inflaton field. The evolution of RHNs number densities n_{N_i} is governed by the Boltzmann equation,

$$\frac{dn_{N_i}}{dt} + 3Hn_{N_i} = R^{\phi^n}_{N_i}, \qquad (50)$$

where $R^{\phi^n}_{N_i}$ is the production rate of RHNs that we will mention in a moment. Defining the comoving number density as $Y_{N_i} = n_{N_i} a^3$, we can re-cast the Boltzmann equation as

$$\frac{dY^T_{N_i}}{da} = \frac{a^2}{H} R^{\phi^n}_{N_i}. \qquad (51)$$

The energy density of inflaton and radiation, on the other hand, evolves as

$$\frac{d\rho_\phi}{dt} + 3H(1 + w_\phi)\rho_\phi = -(1 + w_\phi)\Gamma_\phi \rho_\phi,$$
$$\frac{d\rho_R}{dt} + 4H\rho_R = +(1 + w_\phi)\Gamma_\phi \rho_\phi, \qquad (52)$$

[9] This can be further ensured by noting that the thermalization rate $\Gamma^{\rm th} \simeq y_N^2 T/(8\pi)$ remains below the Hubble rate during reheating at $T = M_1$. One can thus safely ignore the washout effects.

where the production rate of radiation is given by [77,79,81]

$$(1+w_\phi)\Gamma_\phi\rho_\phi = R_H^{\phi^n} \simeq \frac{N_h\rho_\phi^2}{16\pi M_P^4}\sum_{\nu=1}^{\infty}2\nu\omega|\mathcal{P}_{2\nu}^n|^2 = \alpha_n M_P^5\left(\frac{\rho_\phi}{M_P^4}\right)^{\frac{5n-2}{2n}}, \quad (53)$$

where $N_h = 4$ is the number of internal degrees of freedom for one complex Higgs doublet, and we have neglected the Higgs boson mass. Here $\sum_{\nu=1}^{\infty}2\nu\omega|\mathcal{P}_{2\nu}^n|^2$ parametrizes the periodicity of oscillation of the inflaton potential. The values of α_n are computed following [77,78], and are given in Table I. Note that, to avoid conflict with the BBN that requires the reheating temperature $T_{\rm RH} \gtrsim 1$ MeV, one needs to consider[10] $w_\phi \gtrsim 0.65$ [77,80] or $n \gtrsim 9$. However, it was shown in [79] that the gravitational wave constraints exclude a reheating with $T_{\rm RH} \gtrsim 2$ MeV with minimal gravitational coupling. It is then interesting to know if gravitational leptogenesis is possible in the minimal case (pure exchange of a graviton) in the presence of PBH as the source of reheating. Both productions (from inflaton and from PBHs) being gravitational, they can be considered unavoidable sources of baryonic asymmetry in the early Universe. This should open a new window on the parameter space analyzed in the previous section.

The production rate for N_1 from inflaton scattering mediated by gravity is given by [79]

$$R_{N_1}^{\phi^n} = \frac{\rho_\phi^2}{4\pi M_P^4}\frac{M_{N_i}^2}{m_\phi^2}\Sigma_{N_i}^n, \quad (54)$$

where

$$\Sigma_{N_i}^n = \sum_{\nu=1}^{+\infty}|\mathcal{P}_{2\nu}^n|^2\frac{m_\phi^2}{E_{2n}^2}\left(1-\frac{4M_{N_1}^2}{E_{2\nu}^2}\right)^{3/2}, \quad (55)$$

accounts for the sum over the Fourier modes of the inflaton potential, and $E_\nu = \nu\omega$ is the energy of the nth inflaton oscillation mode. The full expression for the inflaton mass m_ϕ can be found in Appendix D.

Since we are only concerned about N_1 production, the comoving number density of N_1 during the postinflationary era is given by

$$\frac{dY_{N_1}^{\phi^n}}{da} = a_{\rm end}^2\frac{\sqrt{3}M_{N_1}^2 M_P}{4\pi n(n-1)\lambda^{\frac{2}{n}}}\left(\frac{\rho_{\rm end}}{M_P^4}\right)^{\frac{n+4}{2n}}\left(\frac{a}{a_{\rm end}}\right)^{-\frac{n+8}{n+2}}\Sigma_{N_1}^n, \quad (56)$$

where we have considered the fact that the Hubble expansion has the dominant contribution from inflaton energy density during reheating. Integrating Eq. (56) between $a_{\rm end}$ and a leads to RHN number density as

$$n_{N_1}^{\phi^n}(a) \simeq \frac{M_{N_1}^2 M_P\sqrt{3}(n+2)}{24\pi n(n-1)\lambda^{\frac{2}{n}}}\left(\frac{\rho_{\rm end}}{M_P^4}\right)^{\frac{n+4}{2n}}\left(\frac{a}{a_{\rm end}}\right)^{-3}\Sigma_{N_1}^n, \quad (57)$$

for $a \gg a_{\rm end}$.

For $\beta < \beta_{\rm c}$, as the inflaton energy density dominates for $a_{\rm end} \ll a < a_{\rm RH}$, we then obtain

$$n_{N_1}^{\phi^n}(a_{\rm RH})|_{\beta<\beta_c} \simeq \frac{M_{N_1}^2\sqrt{3}(n+2)\rho_{\rm RH}^{\frac{1}{2}+\frac{2}{n}}}{24\pi n(n-1)\lambda^{\frac{2}{n}}M_P^{1+\frac{8}{n}}}\left(\frac{\rho_{\rm end}}{\rho_{\rm RH}}\right)^{\frac{1}{n}}\Sigma_{N_1}^n. \quad (58)$$

On the other hand, for $\beta > \beta_{\rm c}$, there is an intermediate PBH-dominated phase before evaporation (reheating) that leads to

$$n_{N_1}^{\phi^n}(a_{\rm RH})|_{\beta>\beta_c} \simeq \frac{M_{N_1}^2 M_P(n+2)48^{\frac{1}{n}}}{8\pi n(n-1)\lambda^{\frac{2}{n}}\beta}\left(\frac{\rho_{\rm end}}{M_P^4}\right)^{\frac{1}{n}} \times\left(\frac{M_P}{M_{\rm in}}\right)^{\frac{2+5n}{n}}\epsilon^2(\pi\gamma)^{-1+\frac{2}{n}}\Sigma_{N_1}^n. \quad (59)$$

Note that for PBH domination, the number density has explicit β dependence, which is expected since β controls the PBH-dominated phase. The final asymmetry in the case of minimal gravitational leptogenesis thus becomes

$$\frac{Y_B(T_0)}{8.7\times10^{-11}} \simeq \delta_{\rm eff}\left(\frac{m_{\nu,\rm max}}{0.05\ {\rm eV}}\right)\frac{M_{N_1}}{1.1\times10^8\ {\rm GeV}}\frac{n_{N_1}^{\phi^n}(a_{\rm RH})}{T_{\rm RH}^3}, \quad (60)$$

where for $\beta < \beta_{\rm c}$,

$$\frac{n_{N_1}^{\phi^n}(a_{\rm RH})}{T_{\rm RH}^3} = \frac{\alpha_T^{\frac{n+2}{2n}}\sqrt{3}(n+2)}{24\pi n(n-1)\lambda^{\frac{2}{n}}}\left(\frac{M_{N_1}}{M_P}\right)^2\left(\frac{T_{\rm RH}}{M_P}\right)^{\frac{4-n}{n}}\left(\frac{\rho_{\rm end}}{M_P^4}\right)^{\frac{1}{n}}\Sigma_{N_1}^n. \quad (61)$$

To compute $T_{\rm RH}$ appearing in Eq. (61), one needs to compute the density of energy when the radiation produced by the PBH decay at $a_{\rm ev}$ dominates over the

TABLE I. Relevant coefficients α_n for the gravitational leptogenesis [cf. Eq. (53)].

n	α_n
6	0.000193
8	0.000528
10	0.000966
12	0.00144

[10]This requirement of having large w_ϕ can be relaxed with nonminimal gravitational couplings as discussed in [77,78,81].

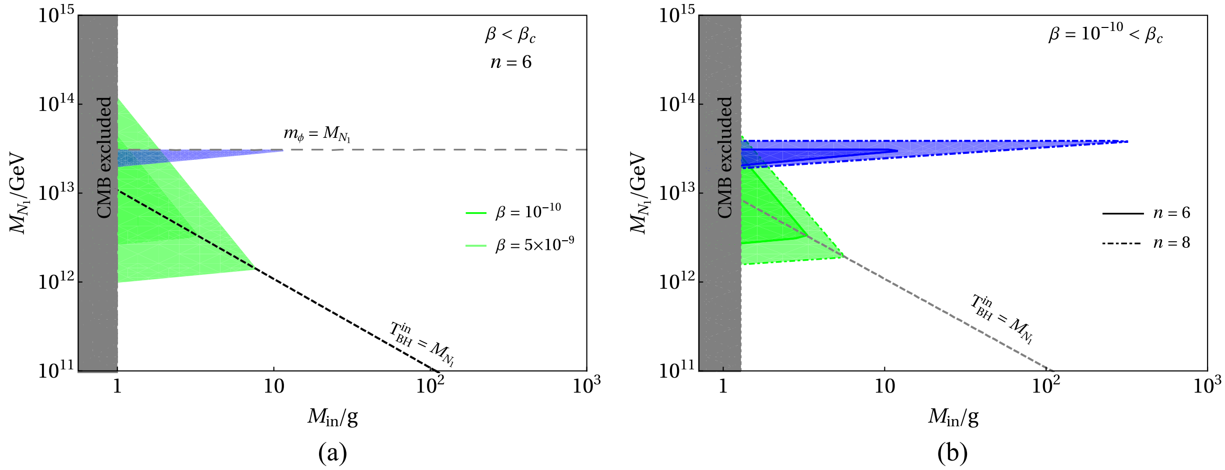

FIG. 7. Inside the blue shaded region, the observed baryon asymmetry is obtained when only gravitational contribution from inflaton scattering is taken into account. In the left panel, we choose $n = 6$ while considering two representative values of β. In the right panel, we choose $\beta = 10^{-10} < \beta_c$ with two different values of $n = \{6, 8\}$. In all cases, the green-shaded region corresponds to the viable parameter space for contribution from PBH evaporation alone, the gray-shaded region is forbidden from CMB bound on the scale of inflation [cf. Eq. (1)], and we ensure reheating from PBH evaporation. The gray dashed line in the left panel indicates $m_\phi = M_{N_1}$, which is the kinematical limit for gravitational leptogenesis.

inflaton density. In other words, we need to solve $\rho_{\rm RH} = \rho_{\rm BH}(a_{\rm ev})(\frac{a_{\rm ev}}{a_{\rm RH}})^4 = \rho_\phi(a_{\rm in})(\frac{a_{\rm in}}{a_{\rm RH}})^{3(1+w_\phi)}$. We obtain

$$T_{\rm RH} \propto \beta^{\frac{3(1+w_\phi)}{3w_\phi-1}}\left(\frac{M_P}{M_{\rm in}}\right)^{\frac{3(1-w_\phi)}{2(1-3w_\phi)}}. \tag{62}$$

The details of the calculation is reported in Appendix D [cf. Eq. (D12)]. Note that Eqs. (60) and (61) are also true for reheating happening entirely from inflaton, where a particular coupling y_ϕ between the inflaton and the SM particles determines the reheating temperature [cf. Eq. (D8)].

For $\beta > \beta_c$, we find

$$\frac{n_{N_1}^{\phi^n}(a_{\rm RH})}{T_{\rm RH}^3} = \frac{48^{\frac{1}{n}}\epsilon^{\frac{1}{2}}\alpha_T^{\frac{3}{4}}(n+2)}{16\sqrt{2}\times 3^{\frac{3}{4}}\pi n(n-1)\lambda^{\frac{2}{n}}\beta}\left(\frac{\rho_{\rm end}}{M_P^4}\right)^{\frac{1}{n}} \times\left(\frac{M_{N_1}}{M_P}\right)^2\left(\frac{M_P}{M_{\rm in}}\right)^{\frac{n+4}{2n}}(\pi\gamma)^{-1+\frac{2}{n}}\Sigma_{N_1}^n. \tag{63}$$

Note that, for $\beta < \beta_c$, the PBH reheating scenario is only valid for $n > 4$, as in this case, a faster dilution of the inflaton energy density is required compared to radiation to achieve successful reheating. This is also reflected in Eq. (D12).

In Fig. 7, on top of leptogenesis from PBH evaporation (in green), we show the contribution from minimal gravitational leptogenesis in blue for different values of $\beta < \beta_c$ (left) and different value of n (right). This plot includes the dominant gravitational sources of baryonic asymmetry in a universe populated by an inflaton field and PBHs. For $\beta > \beta_c$, we find that inflaton gravitational production starts contributing on top of PBH evaporation for very light PBHs, which are in tension with the CMB bound. This can be understood from the fact that as lighter PBHs decay earlier, they cause less entropy dilution to the asymmetry compared to heavier PBHs that have longer lifetime. Therefore, for $\beta > \beta_c$, gravitational leptogenesis is important when the PBH mass is typically $\lesssim 1$ g. We, therefore refrain from showing the resulting parameter space for $\beta > \beta_c$ in Fig. 7.

For $\beta < \beta_c$, we see that minimal gravitational leptogenesis from inflaton scattering is more important for lighter PBHs. Combining Eqs. (60) and (62), we can write $Y_B^0 \propto M_N^3 \times M_{\rm in}^{-\frac{3}{n}}$, which corresponds to $M_N \propto M_{\rm in}^{-3/8} M_N^3$ for $n = 8$, which is what we effectively observe in the figure. This comes from the fact that when inflaton dominates the energy budget of the Universe, the reheating temperature due to PBH evaporation evolves as $M_{\rm in}^{\frac{3}{n-4}}$, which one can see from Eq. (62). Following Eq. (61), a lighter $M_{\rm in}$ implies lower reheating temperature, leading to larger yields. For the dependence on β, we note that $Y_B^0 \propto M_{\rm in}^{-3/n}\beta^{-3/4}$, using Eq. (61), together with Eq. (62). Therefore, for a given β, gravity-mediated leptogenesis becomes significant for lighter PBHs when $\beta < \beta_c$. While the inflaton generates a sufficient amount of asymmetry, the PBH ensures a viable reheating if $y_\phi < y_\phi^c$. In every case, the RHN mass is restricted to lie in the range 5×10^{11} GeV $\lesssim M_{N_1} \lesssim 10^{14}$ GeV when taking into account both (PBH and inflaton) contributions. Notably, gravitational leptogenesis is kinematically viable only when $m_\phi > M_{N_1}$, as denoted by the gray dashed line in the left panel.

IV. PRIMORDIAL GRAVITATIONAL WAVE FROM INFLATION

Gravitational waves are transverse ($\partial_i h_{ij} = 0$) and traceless ($h_{ii} = 0$) metric perturbations $ds^2 = a^2(t)(dt^2 - (\delta_{ij} + h_{ij})dx^i dx^j)$. Their energy density spectrum (at subhorizon scales) is defined as [92,115–117]

$$\Omega_{\rm GW}(t,k) \equiv \frac{1}{\rho_{\rm crit}}\frac{d\rho_{\rm GW}(t,k)}{d\ln k} = \frac{k^2}{12a^2(t)H^2(t)}\Delta_h^2(t,k), \quad (64)$$

where $\Delta_h^2(t,k)$ is the tensor power spectrum at arbitrary times, defined by

$$\langle h_{ij}(t,\mathbf{x})h^{ij}(t,\mathbf{x})\rangle \equiv \int \frac{dk}{k}\Delta_h^2(t,k), \quad (65)$$

with $\langle\ldots\rangle$ denoting an average over a statistical ensemble. One can factorize the tensor power spectrum as [92]

$$\Delta_h^2(t,k) \equiv T_h(t,k)\Delta_{h,\rm inf}^2(k), \quad (66)$$

with $T_h(t,k)$ being the transfer function

$$T_h(t,k) = \frac{1}{2}\left(\frac{a_{\rm hc}}{a}\right)^2, \quad (67)$$

where the factor of $1/2$ appears due to the average over the tensor fluctuations. Here "hc" indicates the epoch of horizon reentry (crossing) of a particular mode, and $\Delta_{h,\rm inf}^2(k)$ represents the primordial tensor power spectrum from inflation [92,115],

$$\Delta_{h,\rm inf}^2(k) \simeq \frac{2}{\pi^2}\left(\frac{H_{\rm end}}{M_P}\right)^2\left(\frac{k}{k_p}\right)^{n_t}, \quad (68)$$

with n_t a spectral tilt, k_p a pivot scale of the order the Hubble rate at the time of CMB decoupling, and $H_{\rm end}$ the Hubble rate when the mode k_p exited the Hubble radius during inflation. Since we assume de Sitter-like inflation, the Hubble parameter is the same throughout inflation, and the spectral tilt turns out as $n_t \simeq 0$. Note that such an assumption works fine with any slow-roll model of inflation, such as the $\alpha-$ attractor model of inflation. To determine the energy scale at the end of the inflation, we assume the $\alpha-$ attractor model of inflation as a sample model [for the form of the potential, see Eq. (D4) in Appendix D]. Most of the slow-roll model of inflation (including the one we are considering) behaves as ϕ^{2n} at the minima, and the average inflaton equation of state can be written as $w_\phi = (n-1)/(n+1)$. More specifically, the value of w_ϕ only depends on the behavior of the inflationary potential at the minima, which is related to the postinflationary behavior of the potential. Hence, it can not capture any details of the inflationary model on large scales. Let us assume for a moment that, immediately after inflation, the Universe became radiation-dominated. The resulting GW energy density spectrum at the present epoch would then be scale-invariant for the frequency range corresponding to the modes crossing the Hubble radius during RD. However, if prior to RD, there is a nonstandard phase, say reheating, the resulting present-day GW energy density spectrum consists of two parts; a tilted branch, corresponding to the modes that crossed the horizon during reheating, and a scale-invariant branch corresponding to the modes that crossed the horizon during RD. The spectral tilt

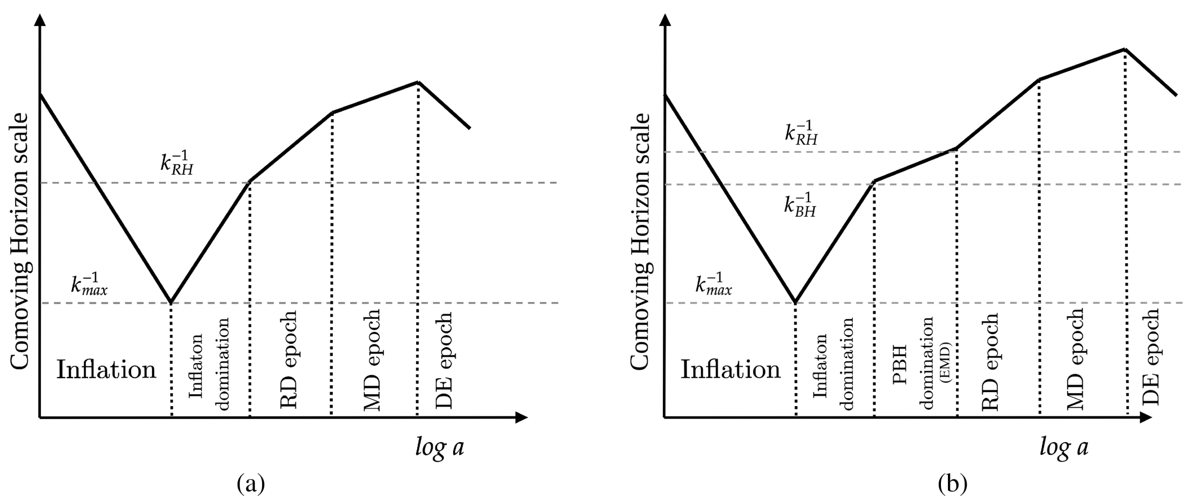

FIG. 8. Schematic diagram showing the evolution of the comoving horizon scale $1/aH$ from inflation till today with respect to the scale factor. In the left panel, we consider $\beta < \beta_c$, while in the right $\beta > \beta_c$. Here "RD", "MD", and "DE" stand respectively for standard radiation domination, late matter domination, and dark energy. In the right panel "EMD" in parenthesis stands for early matter domination, corresponding to the PBH domination epoch. We also denote momenta corresponding to different epochs via the gray dashed horizontal lines.

of the PGW spectrum takes the form $n_{\rm GW} = \frac{6w_\phi-2}{1+3w_\phi}$ [118,119] that predicts a red-tilted spectrum for an EOS $w_\phi < 1/3$, blue-tilted for $w_\phi > 1/3$ and a scale-invariant spectrum for $w_\phi = 1/3$.

In our present analysis, depending on β value, we have two different scenarios as depicted in Fig. 8:

(i) For $\beta < \beta_c$, the Universe does not go through any PBH domination,

$$\text{Inflation} \rightarrow \text{Reheating} \rightarrow \text{Radiation domination;}$$

(ii) For $\beta > \beta_c$, on the other hand, we have

$$\text{Inflation} \rightarrow \text{Inflaton domination} \\ \rightarrow \text{PBH domination} \rightarrow \text{Radiation domination.}$$

In case when there is *no PBH domination* (i.e., the first case listed above), the GW spectral energy density[11] at the present epoch can be represented in a piecewise function of frequency (momenta k) as follows:

$$\Omega^{(0)}_{\rm GW} \simeq \Omega^{(0)}_{\rm GW,rad} \begin{cases} 1 & k < k_{\rm RH} \\ \frac{\zeta}{\pi}\left(\frac{k}{k_{\rm RH}}\right)^{\frac{6w_\phi-2}{1+3w_\phi}} & k_{\rm RH} < k < k_{\rm max}, \end{cases} \tag{69}$$

where $\Omega^{(0)}_{\rm GW,rad}h^2 = \frac{\Omega_{\rm R}h^2 H^2_{\rm end}}{12\pi^2 M_P^2}$ and

$$\zeta = (1+3w_\phi)^{\frac{4}{1+3w_\phi}}\Gamma^2\left(\frac{5+3w_\phi}{2+6w_\phi}\right). \tag{70}$$

$\Omega_{\rm R}h^2 = 4.16\times10^{-5}$ is the present-day radiation abundance considering both photons and neutrinos. Using the entropy conservation between the end of reheating to the present day, we have the mode that reenters the Hubble radius at the end of reheating,

$$k_{\rm RH} \equiv a_{\rm RH}H_{\rm RH} = \left(\frac{43}{11 g_{\rm RH}}\right)^{\frac{1}{3}}\sqrt{\frac{\alpha_T}{3}}\frac{T_0}{M_P}T_{\rm RH}, \tag{71}$$

where T_0 is the present CMB temperature 2.725. Thus, $k_{\rm RH}$ is simply a function of $T_{\rm RH}$, which can be written as

$$k_{\rm RH} \sim 1.6\ {\rm Hz}\left(\frac{T_{\rm RH}}{10^7\ {\rm GeV}}\right)\left(\frac{g_{\rm RH}}{106.75}\right)^{\frac{1}{6}}. \tag{72}$$

[11]GWs at second order can be sourced by the density fluctuation due to the inhomogeneities in the PBH distribution, which puts a constraint on β, requiring subdominant contribution from GW energy density [120–123]. In our case, we are mainly interested in the scenario with no PBH domination, $\beta < \beta_c$, where such induced GWs spectrum is subdominant. Even for $\beta > \beta_c$, we chose β value close to β_c, where such induced gravitational waves can be neglected.

Since here we are interested in the scenario of PBH reheating without PBH domination, $T_{\rm RH}$ is a function of PBH parameters such as formation mass $M_{\rm in}$ and mass fraction β and takes, as we saw, the following form [cf. Eq. (D12)].

$$T_{\rm RH} \sim \mu\beta^{\frac{3(1+w_\phi)}{4(3w_\phi-1)}}\left(\frac{M_P}{M_{\rm in}}\right)^{\frac{3(1-w_\phi)}{2(1-3w_\phi)}}M_P, \tag{73}$$

where

$$\mu = \left(\frac{48\pi^2}{\alpha_T}\right)^{\frac{1}{4}}\left(\frac{\epsilon}{2(1+w_\phi)\pi\gamma^{3w_\phi}}\right)^{\frac{1}{2(1-3w_\phi)}}. \tag{74}$$

On the other hand, the mode reentering right at the end of inflation is designated as $k_{\rm max}$, where

$$k_{\rm max} = a_{\rm max}H_{\rm end} \simeq k_\star e^{N_\star}, \tag{75}$$

where $\star$ quantities are measured at the CMB pivot scale $k_\star \simeq 0.05\ {\rm Mpc}^{-1}$ and N_* represents the inflationary e-folding number calculated from the end of the inflation to the horizon exit of the CMB pivot scale. Under the assumption that the comoving entropy density is conserved from the end of the reheating to the present day, the expression for N_* takes the following form:

$$N_* = \ln\left[2.5\times10^{39}\left(\frac{H_{\rm end}}{10^{13}\ {\rm GeV}}\right)\frac{\rm GeV}{T_{\rm RH}}\right] - N_{\rm RH}. \tag{76}$$

In the first case, where PBH formed and evaporates in an inflaton-dominated background and is responsible for reheating, one can estimate

$$N_{\rm RH} \simeq \frac{1}{3(1+w_\phi)}\ln\left[\frac{H_{\rm end}}{10^{13}\ {\rm GeV}}\left(\frac{1.5\times10^{12}\ {\rm GeV}}{T_{\rm RH}}\right)^4\right]. \tag{77}$$

On the other hand, if there is an intermediate epoch of PBH domination before the reheating ends (i.e., the second case), the GW spectrum shows a red-tilted behavior ($\propto k^{-2}$) for all GW momenta modes that reenter the horizon during the period $k_{\rm BH} < k < k_{\rm RH}$. The final GW spectral energy density at the present epoch then takes the form

$$\Omega^{(0)}_{\rm GW} \simeq \Omega^{(0)}_{\rm GW,rad} \begin{cases} 1 & k < k_{\rm RH} \\ c_1\left(\frac{k}{k_{\rm RH}}\right)^{-2} & k_{\rm BH} < k < k_{\rm RH} \\ c_2\left(\frac{k}{k_{\rm BH}}\right)^{\frac{6w_\phi-2}{1+3w_\phi}} & k_{\rm BH} < k < k_{\rm max}, \end{cases} \tag{78}$$

where $c_1 = [\Gamma(\frac{5}{2})]^2/\pi$, $c_2 = (c\zeta/\pi))(k_{RH}/k_{\rm BH})^2$, and $k_{\rm BH} = k_{\rm max}(a_{\rm BH}/a_{\rm end})^{-(1+3w_\phi)/2}$.

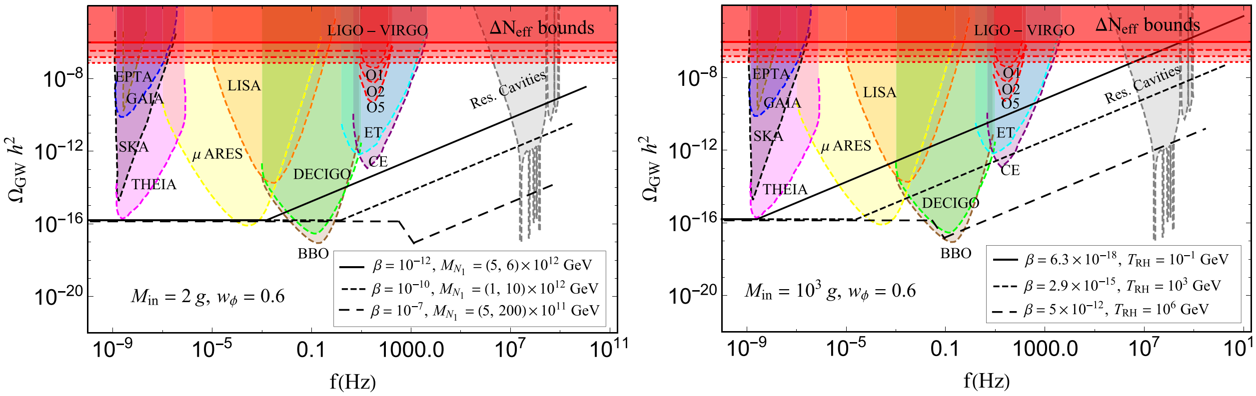

FIG. 9. Left: Spectrum of primordial GW as a function of the frequency f shown via the black curves, for different choices of β and M_{N_1} that satisfy the observed baryon asymmetry. We fix $M_{\rm in} = 2$ g and $w_\phi = 0.6$. Right: Same as left, but for $M_{\rm in} = 10^3$ g and $w_\phi = 0.6$. In both plots, we also show projections from present and future GW experiments, together with the existing and projected $\Delta N_{\rm eff}$ bounds (labeled as "$\Delta N_{\rm eff}$ bounds").

In Fig. 9, we show the spectrum of primordial GW as a function of the frequency, along with the current and future sensitivities of various GW experiments, like, LIGO [124–129], LISA [130,131], CE [132,133], ET [134,135], BBO [104,105], DECIGO [107,136–139], μ-ARES [140], and THEIA [141],[12] that search for signals in the low frequency (kHz) regions. We also project sensitivity from proposed high frequency GW experiments, e.g., resonant cavities [142,143] that typically look for GW signals in GHz–MHz frequency regime.

In the left panel of Fig. 9 we show GW spectrum corresponding to different choices of β, for a fixed M_{N_1} with a given $M_{\rm in} = 2$ g and $w_\phi = 0.6$. Note that, for these choices of the RHN masses one can satisfy the observed baryon asymmetry by exploiting the Casas-Ibarra parametrization. The noteworthy feature here is the scale-invariant spectrum, followed by a blue-tilted branch in case of $\beta < \beta_c$. This, as explained before, is because of the presence of stiff equation of state during reheating, when PBH domination is absent. For $\beta > \beta_c$, we see the effect of intermediate PBH-domination (black-dashed curve) that gives rise to red-tilted spectrum. In the right panel, we see similar behavior of the GW spectrum, but now with different choices of $T_{\rm RH}$, for $M_{\rm in} = 10^3$ g and $w_\phi = 0.6$. In both panel the horizontal lines, along with the shaded region marked as "$\Delta N_{\rm eff}$ bound" collectively shows present and future bounds from $\Delta N_{\rm eff}$ from different experiments which we are going to explain in the very next section.

A. Constraints from $\Delta N_{\rm eff}$

Any extra radiation component, in addition to those of the SM, can be expressed in terms of the $\Delta N_{\rm eff}$. This can be done by computing the total radiation energy density in the late Universe as

$$\rho_{\rm rad} = \rho_\gamma + \rho_\nu + \rho_{\rm GW} = \left[1 + \frac{7}{8}\left(\frac{T_\nu}{T_\gamma}\right)^4 N_{\rm eff}\right]\rho_\gamma, \tag{79}$$

where ρ_γ, ρ_ν, and $\rho_{\rm GW}$ correspond to the photon, SM neutrino, and GW energy densities, respectively, with $T_\nu/T_\gamma = (4/11)^{1/3}$. Within the SM, taking the noninstantaneous neutrino decoupling into account, one finds $N_{\rm eff}^{\rm SM} = 3.044$ [144–152], while the presence of GW results in a modification,

$$\Delta N_{\rm eff} = N_{\rm eff} - N_{\rm eff}^{\rm SM} = \frac{8}{7}\left(\frac{11}{4}\right)^{\frac{4}{3}}\left(\frac{\rho_{\rm GW}(T)}{\rho_\gamma(T)}\right). \tag{80}$$

The above relation can be utilized to put a constraint on the GW energy density redshifted to today via [88,92,153]

$$\int_{k_{\rm BBN}}^{k_{\rm max}} \frac{dk}{k}\,\Omega_{\rm GW}^{(0)} h^2(k) \leq \frac{7}{8}\left(\frac{4}{11}\right)^{4/3} \Omega_\gamma h^2 \Delta N_{\rm eff}, \tag{81}$$

where $\Omega_\gamma h^2 \simeq 2.47\times 10^{-5}$ is the relic density of the photon today.

The $\Delta N_{\rm eff}$ constraints on the GW spectral energy density become relevant when the PBHs evaporate in an inflaton-dominated background. Therefore, for a background equation of state $w_\phi > 1/3$, the blue tilted nature of the spectrum becomes apparent with maximum momenta $k_{\rm max}$ for the mode that reenters the horizon right at the end of the inflation. In this case Eq. (81) takes the form,

$$\int_{k_{\rm BBN}}^{k_{\rm max}} \frac{dk}{k}\,\Omega_{\rm GW}^{(0)} h^2(k) \simeq \Omega_{\rm GW,rad}^{(0)} h^2 \mu \left(\frac{k_{\rm max}}{k_{\rm RH}}\right)^{\frac{6w_\phi - 2}{1+3w_\phi}}, \tag{82}$$

where $\mu = \frac{\zeta(1+3w_\phi)}{2\pi(3w_\phi - 1)}$. Assuming a w_ϕ dominated phase between inflation and radiation domination (no PBH

[12]Here we have used the sensitivity curves derived in Ref. [141].

TABLE II. Present and future constraints on $\Delta N_{\rm eff}$ from different experiments.

$\Delta N_{\rm eff}$	Experiments
0.17	Planck legacy data (combining BAO) [4]
0.14	BBN+CMB combined [157]
0.06	CMB-S4 [158]
0.027	CMB-HD [159]
0.013	COrE [160], Euclid [161]
0.06	PICO [162]

domination), the ratio between $k_{\rm max}$ and $k_{\rm RH}$ can be expressed as

$$\frac{k_{\rm max}}{k_{\rm RH}} = \left(\frac{\rho_{\rm end}}{\alpha_T}\right)^{\frac{1+3w_\phi}{6(1+w_\phi)}} T_{\rm RH}^{-\frac{2}{3}\frac{(1+3w_\phi)}{(1+w_\phi)}}. \tag{83}$$

Upon substitution of the above equation into Eq. (82) and utilizing Eq. (81), one can find the restriction on the reheating temperature,

$$T_{\rm RH} \geq \left(\frac{\Omega^{(0)}_{\rm GW,rad} h^2 \mu}{5.61\times 10^{-6}\Delta N_{\rm eff}}\right)^{\frac{3(1+w_\phi)}{4(3w_\phi-1)}} \times \left(\frac{\rho_{\rm end}}{\alpha_T}\right)^{\frac{1}{4}}, \tag{84}$$

where $\rho_{\rm end}$ is the energy density of the inflaton at the end of the inflation, $\rho_{\rm end} = 3M_P^2 H_{\rm end}^2$. Since we are interested in the PBH reheating scenario (no PBH domination), the above restriction on the reheating temperature, in turn, puts bounds on the PBH parameter [cf. Eq. (73)] via

$$\beta \geq \left(\frac{\Omega^{(0)}_{\rm GW,rad} h^2 \mu}{5.61\times 10^{-6}\Delta N_{\rm eff}}\right)\left(\frac{M_P}{M_{\rm in}}\right)^{\frac{2(1-w_\phi)}{1+w_\phi}}\left(\frac{1}{\mu^4\alpha_{\rm T}}\frac{\rho_{\rm end}}{M_P^4}\right)^{\frac{3w_\phi-1}{3(1+w_\phi)}}. \tag{85}$$

Note that the above restriction is only important when TRH > TBBN= 4 MeV [154–156], otherwise, BBN provides a stronger bound than $\Delta N_{\rm eff}$. In Table II, we tabulate present and future bounds on $\Delta N_{\rm eff}$ from different experiments as mentioned. These bounds are projected in Fig. 9, from where we see that lower reheating temperatures are typically in conflict with these bounds, as seen from the right panel of Fig. 9. The $\Delta N_{\rm eff}$ bound on the translated into a bound on PBH mass and β-value following Eq. (85). This is shown in Fig. 10, where we use the present bound on $\Delta N_{\rm eff}$ from Planck [4]. We see the available parameter space is more tightly constrained for heavier PBH in the case of a stiffer fluid (i.e., a larger equation of state). As one can see from Eq. (85), the bound becomes independent of PBH mass as $w_\phi \to 1$, i.e., pure kination. Note that the $\Delta N_{\rm eff}$ bound for the contribution from the PGWs is only important when $w_\phi > 0.60\,(n > 8)$ [102]. Thus, our presented results are safe from such restrictions.

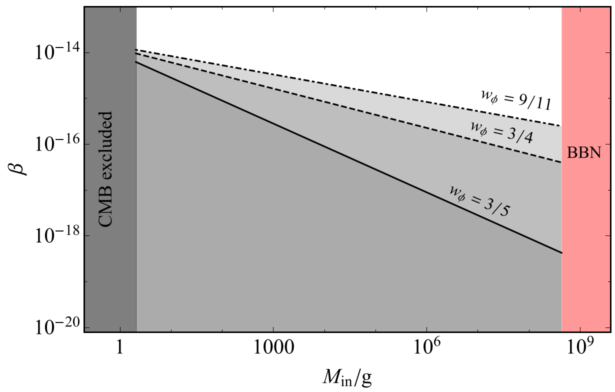

FIG. 10. Constraint from $\Delta N_{\rm eff}$ in $\beta - M_{\rm in}$ plane for different choices of the background equation of states w_ϕ. All shaded regions are excluded (see text for details).

V. CONCLUSIONS

The observed baryon asymmetry of the Universe can be produced via leptogenesis, which requires extending the Standard Model (SM) particle content with the addition of RHNs, singlet under the SM gauge symmetry. Gravitation should produce a minimal unavoidable amount of RHN fields. Once gravitationally produced, these RHNs can then undergo CP-violating decay to produce the lepton and subsequently, the baryon asymmetry.

Pure gravitational production can take place in two ways: (i) from evaporation of PBHs and (ii) scattering of the inflaton (or bath particles), mediated by a massless graviton field. The latter production occurs during reheating when the inflaton field ϕ oscillates around the minima of a monomial potential $V(\phi) \propto \phi^n$, transferring its energy to the thermal bath. In the presence of PBHs, however, the reheating dynamics is controlled not only by the steepness of the potential n and the nature of the inflaton-SM coupling, but also by the PBH mass and the fractional abundance of PBHs. Moreover, for $n > 4$ (or equivalently, a general equation of state $w_\phi > 1/3$), the primordial gravitational waves produced from the tensor perturbations during inflation, are hugely blue-tilted. Such a boosted GW energy density on one hand falls within the sensitivity range of GW detectors, while on the other hand, may also be in tension with excessive production of energy density around BBN.

In the present work, we first compute the amount of baryonic asymmetry Y_B^0 at the present epoch, generated through the gravitational production of RHN. Depending on the relative amount of energy β, the PBHs can lead the reheating process and produce an amount of RHN sufficient to satisfy the constraint on Y_B^0. However, this is possible only for very light PBH $\lesssim 10$ g, as one can see in Fig. 2. If PBHs do not dominate the energy budget of the Universe at the time of reheating, the situation worsens due to an excessive entropy dilution, as it is clear from Fig. 5, plotted for smaller values of β. For a complete picture, one has also included the other gravitational source of RHNs, i.e., the inflation scattering through graviton exchange. In this scenario, a new region of the parameter space opens up with larger PBH masses, as one can see from Fig. 7. In any case, the allowed mass range for the RHN remains 5×10^{11} GeV $\lesssim M_{N_1} \lesssim 5\times10^{14}$ GeV. Too-light RHNs do not generate a sufficient amount of asymmetry, while too-heavy RHNs are not sufficiently produced by inflaton scattering or from PBH evanescence.

It is then possible to find signatures of different reheating, as well as gravitational production scenarios (inflaton or PBH sourced) through GW observations. We exploit the blue-tilted nature of primordial GW in probing the scale of nonthermal gravitational leptogenesis during reheating. The reheating via inflaton is controlled by the Yukawa coupling between the inflaton and a pair of SM-like fermions, *viz.*, $y_\phi \phi f \bar{f}$. PBHs, however, are assumed to be formed during the epoch of reheating and are parametrized by their formation mass $M_{\rm in}$ and initial abundance β. Depending on the values of $\{y_\phi, M_{\rm in}, \beta, n\}$, PBHs can potentially impact the reheating process and populate the thermal bath. In Fig. 9, we delineate the parameter space that agrees with the observed baryon asymmetry, considering RHN production takes place during reheating both from PBH evaporation and from the scattering of inflaton condensate (mediated by graviton).

For a stiff equation of state for the background ϕ (large n), we observe that the spectrum of primordial GW lies well within reach of future GW detectors [cf. Fig. 9], both in the low frequency (kHz) and in the high-frequency (GHz) regime, satisfying bounds from $\Delta N_{\rm eff}$, as one can see from Figs. 9 and 10. Interestingly, the *red-tilted* GW spectrum that exists because of the intermediate PBH domination (for $\beta > \beta_c$), also turns out to be within the reach of futuristic GW detectors. The present scenario therefore provides a window to test modified cosmological background prior to BBN, induced by inflaton and PBH dynamics, together with purely gravitational leptogenesis through primordial GW spectrum.

ACKNOWLEDGMENTS

This project has received support from the European Union's Horizon 2020 research and innovation program under the Marie Sklodowska-Curie grant agreement No. 860881-HIDDeN and the CNRS-IRP project UCMN. B. B. would like to acknowledge the "Planck 2023" conference at the University of Warsaw, during which discussions regarding this work was initiated. S. J. D. is supported by IBS under the Project Code No. IBS-R018-D1. S. J. D. would also like to thank the support and hospitality of the Tata Institute of Fundamental Research (TIFR), Mumbai, where a part of this project was carried out. M. R. H. wishes to acknowledge support from the Science and Engineering Research Board (SERB), Government of India (GoI), for the SERB National Post-Doctoral fellowship, File Number: PDF/2022/002988.

APPENDIX A: THE BOLZMANN EQUATIONS FOR PBH-INFLATON-RADIATION SYSTEM

In order to track the evolution of radiation (ρ_R), PBH ($\rho_{\rm BH}$), and inflaton (ρ_ϕ) energy densities, together with number density of right-handed neutrinos (n_N), the asymmetry $B-L$ and the Hubble parameter H, we solve the following set of Boltzmann equations numerically:

$$\begin{aligned}
\frac{d\rho_\phi}{da} + 3(1+w_\phi)\frac{\rho_\phi}{a} &= -\frac{\Gamma_\phi}{H}(1+w_\phi)\frac{\rho_\phi}{a},\\
\frac{d\rho_R}{da} + 4\frac{\rho_R}{a} &= -\frac{\rho_{\rm BH}}{M_{\rm BH}}\frac{dM_{\rm BH}}{da} + \frac{\Gamma_\phi\rho_\phi(1+w_\phi)}{aH},\\
\frac{d\rho_{\rm BH}}{da} + 3\frac{\rho_{\rm BH}}{a} &= \frac{\rho_{\rm BH}}{M_{\rm BH}}\frac{dM_{\rm BH}}{da},\\
\frac{dn_{N_1}^{\rm BH}}{da} + 3\frac{n_{N_1}^{\rm BH}}{a} &= -n_{N_1}^{\rm BH}\Gamma_{N_1}^{\rm BH} + \Gamma_{{\rm BH}\to N_1}\frac{\rho_{\rm BH}}{M_{\rm BH}}\frac{1}{aH},\\
\frac{dn_{B-L}}{da} + 3\frac{n_{B-L}}{a} &= \frac{\kappa_{\Delta L}}{aH}[(n_{N_1}^T - n_{N_1}^{\rm eq})\Gamma_{N_1}^T + n_{N_1}^{\rm BH}\Gamma_{N_1}^{\rm BH}],\\
\frac{dM_{\rm BH}}{da} &= -\epsilon\frac{M_P^4}{M_{\rm BH}^2}\frac{1}{aH},\\
H^2 &= \frac{\rho_\phi+\rho_R+\rho_{\rm BH}}{3M_P^2}.
\end{aligned} \tag{A1}$$

Here the 'T' and 'BH' stands for thermal and PBH (nonthermal) contributions, respectively. We define $\Gamma_N^{\rm BH}$ as the decay width corrected by an average time dilation factor,

$$\Gamma_N^{\rm BH} = \left\langle\frac{M_N}{E_N}\right\rangle_{\rm BH}\Gamma_N \approx \frac{K_1(M_N/T_{\rm BH})}{K_2(M_N/T_{\rm BH})}\Gamma_N, \tag{A2}$$

where $K_{1,2}[\ldots]$ are the modified Bessel functions of second kind and the thermal average is obtained assuming that the Hawking spectrum has a Maxwell-Boltzmann form, while

$$\Gamma_N = \frac{M_N}{8\pi}y_N^\dagger y_N \tag{A3}$$

is the total decay RHN decay width, with y_N being parametrized following Eq. (B4). Here $\Gamma_{{\rm BH}\to N_1}$ is the nonthermal production term for RHNs (originating from PBH evaporation) and can be written as

$$\begin{aligned}
\Gamma_{{\rm BH}\to N_1} &= \int\frac{d^2\mathcal{N}}{dp\,dt}dp\\
&\approx \frac{27T_{\rm BH}}{32\pi^2}[-z_{\rm BH}{\rm Li}_2(-e^{-z_{\rm BH}}) - {\rm Li}_3(-e^{-z_{\rm BH}})],
\end{aligned} \tag{A4}$$

where ${\rm Li}_s[\ldots]$ are polylogarithm functions of order s; assuming the graybody factor equal to the geometric optics limit, such analytical expression is obtained. In Fig. 11 we show the evolution of energy densities and the $B-L$

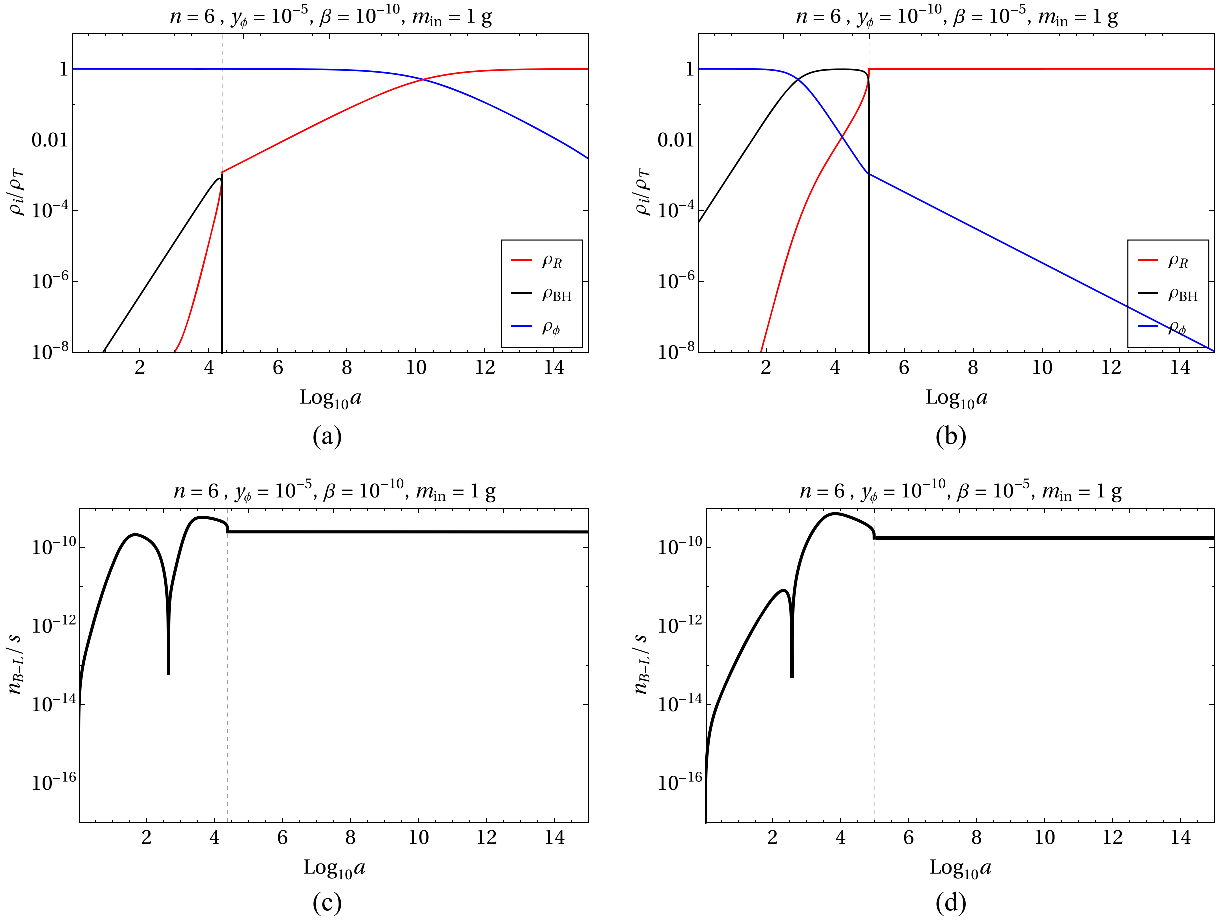

FIG. 11. (a), (b) Evolution of radiation (red), inflaton (blue), and PBH (black) energy densities with the scale factor, obtained by numerically solving Eq. (A1). (c), (d) Evolution of n_{B-L}/s as a function of the scale factor. The final asymmetry satisfies the observed value $Y_B^0 \simeq 8.7 \times 10^{-11}$. All relevant parameters are mentioned in the plot legend.

asymmetry as a function of the scale factor for two benchmark values of y_ϕ and β such that in one case (top-left panel) inflaton dominates the reheating process, while in the other (top-right panel) it is dominated by the PBH.

APPENDIX B: CASAS-IBARRA PARAMETERIZATION

As the neutral component of the SM Higgs doublet acquires a vacuum expectation value leading to the spontaneous breaking of the SM gauge symmetry, neutrinos in the SM obtain a Dirac mass that can be written as

$$m_D = \frac{y_N}{\sqrt{2}} v. \tag{B1}$$

The Dirac mass m_D together with the RHN bare mass M_N, can explain the nonzero light neutrino masses with the help of Type-I seesaw [163–165]. Here, the light-neutrino masses can be expressed as

$$m_\nu \simeq m_D^T M^{-1} m_D. \tag{B2}$$

The mass eigenvalues and mixing are then obtained by diagonalizing the light-neutrino mass matrix as

$$m_\nu = \mathcal{U}^* m_\nu^d \mathcal{U}^\dagger, \tag{B3}$$

with $m_\nu^d = \mathrm{diag}\{m_{\nu_1}, m_{\nu_2}, m_{\nu_3}\}$, consisting of the mass eigenvalues and $\mathcal{U}$ being the Pontecorvo-Maki-Nakagawa-Sakata matrix [166].[13] In order to obtain a complex structure of the Yukawa coupling which is essential from the perspective of leptogenesis, we use the well-known Casas-Ibarra (CI) parametrization [167]. Using this one can write the Yukawa coupling y_N as

$$y_N = \frac{\sqrt{2}}{v} \sqrt{M} \mathbb{R} \sqrt{m_\nu^d} \mathcal{U}^\dagger, \tag{B4}$$

where $\mathbb{R}$ is a complex orthogonal matrix $\mathbb{R}^T \mathbb{R} = I$, which we choose as

[13]The charged lepton mass matrix is considered to be diagonal.

$$\mathbb{R} = \begin{pmatrix} 0 & \cos z & \sin z \\ 0 & -\sin z & \cos z \end{pmatrix}, \tag{B5}$$

where $z = a + ib$ is a complex angle. The digonal light neutrino mass matrix m_ν^d is calculable using the best-fit values obtained from the latest neutrino oscillation data [166]. The elements of Yukawa coupling matrix y_N for a specific value of z, can be obtained for different choices of the heavy neutrino masses.

APPENDIX C: EXPRESSION FOR THE *CP* ASYMMETRY

The CP asymmetry generated from N_1 decay is given by [61]

$$\kappa_{\Delta L} \equiv \frac{\Gamma_{N_1\to \ell_i H} - \Gamma_{N_1\to \bar{\ell}_i \bar{H}}}{\Gamma_{N_1\to \ell_i H} + \Gamma_{N_1\to \bar{\ell}_i \bar{H}}} \simeq \frac{1}{8\pi}\frac{1}{(y_N^\dagger y_N)_{11}} \times \sum_{j=2,3} \mathrm{Im}(y_N^\dagger y_N)_{1j}^2 \times \mathcal{F}\left(\frac{M_j^2}{M_1^2}\right), \tag{C1}$$

where

$$\mathcal{F}(x) \equiv \sqrt{x}\left[\frac{1}{1-x} + 1 - (1+x)\log\left(\frac{1+x}{x}\right)\right]. \tag{C2}$$

For $x \gg 1, \mathcal{F} \simeq -3/(2\sqrt{x})$, and Eq. (C1) becomes

$$\kappa_{\Delta L} \simeq -\frac{3}{16\pi}\frac{1}{(y_N^\dagger y_N)_{11}} \times \left[\mathrm{Im}(y_N^\dagger y_N)_{12}^2 \frac{m_{N_1}}{m_{N_2}} + \mathrm{Im}(y_N^\dagger y_N)_{13}^2 \frac{m_{N_1}}{m_{N_3}}\right]. \tag{C3}$$

If we assume $\mathrm{Im}(y_N^\dagger y_N)_{13}^2 \gg \mathrm{Im}(y_N^\dagger y_N)_{12}^2$ and $m_{N_1} \ll m_{N_{2,3}}$, then

$$\kappa_{\Delta L} \simeq -\frac{3\delta_{\mathrm{eff}}}{16\pi}\frac{|(y_N)_{13}|^2 m_{N_1}}{m_{N_3}}, \tag{C4}$$

while the effective CP-violating phase is given by

$$\delta_{\mathrm{eff}} = \frac{1}{(y_N)_{13}^2}\frac{\mathrm{Im}(y_N^\dagger y_N)_{13}^2}{(y_N^\dagger y_N)_{11}}. \tag{C5}$$

In order to simultaneously generate the active neutrino mass, one has to impose the seesaw relation

$$m_{\nu_3} = \frac{|(y_N)_{13}|^2 v^2}{m_{N_3}}, \tag{C6}$$

that leads to

$$\kappa_{\Delta L} \simeq -\frac{3\delta_{\mathrm{eff}}}{16\pi}\frac{m_{N_1} m_{\nu_3}}{v^2}. \tag{C7}$$

Instead, if $\mathrm{Im}(y_N^\dagger y_N)_{13}^2 \ll \mathrm{Im}(y_N^\dagger y_N)_{12}^2$, the CP-asymmetry parameter becomes

$$\kappa_{\Delta L} \simeq -\frac{3\delta_{\mathrm{eff}}}{16\pi}\frac{m_{N_1} m_{\nu_2}}{v^2}. \tag{C8}$$

In general, one can then write

$$\kappa_{\Delta L} \simeq -\frac{3\delta_{\mathrm{eff}}}{16\pi}\frac{m_{N_1} m_{\nu_i}}{v^2}, \tag{C9}$$

where $i = 2, 3$ for normal hierarchy. In a similar fashion, the CP-asymmetry parameter can be obtained for the inverted hierarchy with $i = 1, 2$.

APPENDIX D: DETAILS OF THE REHEATING DYNAMICS

Considering the inflaton-SM interaction of the form $y_\phi \phi \bar{f} f$, where f are the SM-like fermions, we have the radiation energy density as

$$\rho_R^{\mathrm{D}}(a) = \frac{y_\phi^2}{8\pi}\lambda^{\frac{1-w_\phi}{2(1+w_\phi)}} \tilde{\alpha}_n M_P^4 \left(\frac{\rho_{\mathrm{end}}}{M_P^4}\right)^{\frac{3}{2}-\frac{1}{1+w_\phi}} \left(\frac{a}{a_{\mathrm{end}}}\right)^{-4} \times \left[\left(\frac{a}{a_{\mathrm{end}}}\right)^{\frac{5-9w_\phi}{2}} - 1\right], \tag{D1}$$

and

$$\tilde{\alpha}_n = \frac{\sqrt{3n^3(n-1)}}{7-n} M_P^4, \tag{D2}$$

where a_{end} is the scale factor associated with the end of inflation and λ can be expressed in terms of the amplitude of the CMB power spectrum A_s as

$$\lambda \simeq \frac{18\pi^2 A_s}{6^{n/2} N_e^2}, \tag{D3}$$

for the α-attractor potential [168,169] of the form

$$V(\phi) = \lambda M_P^4 \left[\tanh\left(\frac{\phi}{\sqrt{6\alpha} M_P}\right)\right]^n \simeq \lambda M_P^4 \times \begin{cases} 1, & \phi \gg M_P, \\ \left(\frac{\phi}{\sqrt{6\alpha} M_P}\right)^n, & \phi \ll M_P. \end{cases} \tag{D4}$$

Here N_e is the number of e-folds measured from the end of inflation to the time when the pivot scale $k_\star \simeq 0.05\ \mathrm{Mpc}^{-1}$ exits the horizon. In our analysis, we consider $\log(10^{10} A_s) = 0.04$ [170] and set $N_e = 55$.

One can find the effective mass of the inflaton which is defined as the second derivative of the inflaton potential as

$$m_\phi^2(t) = V''(\phi_0(t)) = n(n-1)\lambda M_P^2 \left(\frac{\phi_0(t)}{M_P}\right)^{n-2}. \tag{D5}$$

Assuming that the oscillation's time scale is small compared to the decay and redshift time scales, $\phi_0(t)$ captures the impact of both decay and redshift. The inflaton energy density $\rho_\phi = \langle(\dot\phi^2/2) + V(\phi)\rangle \sim V(\phi_0)$ can be approximated by $\langle\dot\phi^2\rangle \simeq \langle\phi V'(\phi)\rangle$, that is obtained by averaging the single oscillation. With that assumption, the expression for inflaton mass is obtained as

$$m_\phi^2(t) = n(n-1)\lambda^{\frac{2}{n}} M_P^2 \left(\frac{\rho_\phi}{M_P^4}\right)^{\frac{n-2}{n}}. \tag{D6}$$

Defining the end of reheating (onset of radiation domination) as $\rho_\phi(a_{\rm RH}) = \rho_{\rm R}(a_{\rm RH}) = \rho_{\rm RH}$ one finds

$$\frac{a_{\rm RH}}{a_{\rm end}} = \begin{cases} \left[\frac{y_\phi^2}{8\pi}\tilde\alpha_n \left(\frac{\lambda M_P^4}{\rho_{\rm end}}\right)^{\frac{1-w_\phi}{2(1+w_\phi)}}\right]^{\frac{2}{3(w_\phi-1)}}, & n<7 \\ \left[-\frac{y_\phi^2}{8\pi}\tilde\alpha_n \left(\frac{\lambda M_P^4}{\rho_{\rm end}}\right)^{\frac{1-w_\phi}{2(1+w_\phi)}}\right]^{\frac{1}{1-3w_\phi}}, & n>7, \end{cases} \tag{D7}$$

that leads to

$$\rho_{\rm RH}^{\rm D} = \begin{cases} \left(\frac{y_\phi^2}{8\pi}\tilde\alpha_n\right)^{\frac{2(1+w_\phi)}{1-w_\phi}} \mathcal{M}, & n<7 \\ \left(\frac{y_\phi^2}{8\pi}\tilde\alpha_n\right)^{\frac{3(1+w_\phi)}{3w_\phi-1}} \mathcal{M}^{\frac{3(1-w_\phi)}{2(3w_\phi-1)}} \rho_{\rm end}^{\frac{5-9w_\phi}{2(1-3w_\phi)}}, & n>7, \end{cases} \tag{D8}$$

where $\mathcal{M} = \lambda M_P^4$. Now, the radiation energy density at the end of PBH-driven reheating reads

$$\rho_{\rm RH} = \rho_R(a_{\rm ev})\left(\frac{a_{\rm ev}}{a_{\rm RH}}\right)^4 \simeq \rho_{\rm BH}(a_{\rm ev})\left(\frac{a_{\rm ev}}{a_{\rm RH}}\right)^4, \tag{D9}$$

while the inflaton energy density reads

$$\rho_\phi(a_{\rm RH}) = \rho_\phi(a_{\rm in})\left(\frac{a_{\rm in}}{a_{\rm RH}}\right)^{3(1+w_\phi)}. \tag{D10}$$

Upon substitution of Eq. (32) into Eq. (D9) and comparing with (D10), one can find

$$\left(\frac{a_{\rm ev}}{a_{\rm RH}}\right)^4 = \beta^{\frac{4}{3w_\phi-1}}\left(\frac{a_{\rm in}}{a_{\rm ev}}\right)^{\frac{12w_\phi}{1-3w_\phi}}. \tag{D11}$$

Utilizing the above equation, $\rho_{\rm RH}$ can be written as

$$\rho_{\rm RH} = 48\pi^2\beta^{\frac{3(1+w_\phi)}{3w_\phi-1}}\left(\frac{\epsilon}{2(1+w_\phi)\pi\gamma^{3w_\phi}}\right)^{\frac{2}{1-3w_\phi}}\left(\frac{M_P}{M_{\rm in}}\right)^{\frac{6(1-w_\phi)}{1-3w_\phi}} M_P^4. \tag{D12}$$

Imposing the condition that for $y_\phi = y_\phi^c$ one should have $\rho_{\rm RH} = \rho_{\rm RH}^{\rm D}$, we find

$$y_\phi^c = \begin{cases} \sqrt{\frac{8\pi}{\tilde\alpha_n}} \times \beta^{\frac{3(1-w_\phi)}{4(3w_\phi-1)}} \times \mathcal{A}, & n<7 \\ \sqrt{-\frac{8\pi\beta}{\tilde\alpha_n}} \times \left(\frac{\rho_{\rm end}}{M_P^4}\right)^{\frac{5-9w_\phi}{12(1+w_\phi)}} \times \mathcal{B}, & n>7, \end{cases} \tag{D13}$$

where $\mathcal{A} = \left(\frac{48\pi^2}{\lambda}\right)^{\frac{1-w_\phi}{4(1+w_\phi)}}\mathcal{E}^{\frac{1-w_\phi}{2(1-3w_\phi)(1+w_\phi)}} r^{\frac{3}{2}\frac{(1-w_\phi)^2}{(1-3w_\phi)(1+w_\phi)}}$ and $\mathcal{B} = (48\pi^2)^{\frac{3w_\phi-1}{6(1+w_\phi)}}\lambda^{\frac{w_\phi-1}{4(1+w_\phi)}}\mathcal{E}^{-\frac{1}{3(1+w_\phi)}} r^{\frac{1-w_\phi}{1+w_\phi}}$, with $\mathcal{E} = \frac{\epsilon\gamma^{-3w_\phi}}{2\pi(1+w_\phi)}$, $r = M_P/M_{\rm in}$ and $\tilde\alpha_n = \frac{2(1+w_\phi)}{5-9w_\phi}\sqrt{\frac{6(1+w_\phi)(1+3w_\phi)}{(1-w_\phi)^2}}$.

[1] S. W. Hawking, Nature (London) **248**, 30 (1974).
[2] S. W. Hawking, Commun. Math. Phys. **43**, 199 (1975); **46**, 206(E) (1976).
[3] B. Carr and F. Kuhnel, Annu. Rev. Nucl. Part. Sci. **70**, 355 (2020).
[4] N. Aghanim *et al.* (Planck Collaboration), Astron. Astrophys. **641**, A6 (2020); **652**, C4(E) (2021).
[5] L. Morrison, S. Profumo, and Y. Yu, J. Cosmol. Astropart. Phys. 05 (2019) 005.
[6] P. Gondolo, P. Sandick, and B. Shams Es Haghi, Phys. Rev. D **102**, 095018 (2020).
[7] N. Bernal and O. Zapata, J. Cosmol. Astropart. Phys. 03 (2021) 015.
[8] A. M. Green, Phys. Rev. D **60**, 063516 (1999).
[9] M. Y. Khlopov, A. Barrau, and J. Grain, Classical Quantum Gravity **23**, 1875 (2006).
[10] D.-C. Dai, K. Freese, and D. Stojkovic, J. Cosmol. Astropart. Phys. 06 (2009) 023.
[11] R. Allahverdi, J. Dent, and J. Osinski, Phys. Rev. D **97**, 055013 (2018).
[12] O. Lennon, J. March-Russell, R. Petrossian-Byrne, and H. Tillim, J. Cosmol. Astropart. Phys. 04 (2018) 009.
[13] D. Hooper, G. Krnjaic, and S. D. McDermott, J. High Energy Phys. 08 (2019) 001.
[14] A. Chaudhuri and A. Dolgov, arXiv:2001.11219.
[15] I. Masina, Eur. Phys. J. Plus **135**, 552 (2020).
[16] I. Baldes, Q. Decant, D. C. Hooper, and L. Lopez-Honorez, J. Cosmol. Astropart. Phys. 08 (2020) 045.

[17] N. Bernal and O. Zapata, Phys. Lett. B **815**, 136129 (2021).
[18] N. Bernal and O. Zapata, J. Cosmol. Astropart. Phys. 03 (2021) 007.
[19] B. C. Lacki and J. F. Beacom, Astrophys. J. Lett. **720**, L67 (2010).
[20] S. M. Boucenna, F. Kuhnel, T. Ohlsson, and L. Visinelli, J. Cosmol. Astropart. Phys. 07 (2018) 003.
[21] J. Adamek, C. T. Byrnes, M. Gosenca, and S. Hotchkiss, Phys. Rev. D **100**, 023506 (2019).
[22] B. Carr, F. Kuhnel, and L. Visinelli, Mon. Not. R. Astron. Soc. **506**, 3648 (2021).
[23] I. Masina, arXiv:2103.13825.
[24] N. Bernal, Y. F. Perez-Gonzalez, Y. Xu, and O. Zapata, arXiv:2110.04312.
[25] N. Bernal, F. Hajkarim, and Y. Xu, Phys. Rev. D **104**, 075007 (2021).
[26] R. Samanta and F. R. Urban, arXiv:2112.04836.
[27] P. Sandick, B. S. Es Haghi, and K. Sinha, Phys. Rev. D **104**, 083523 (2021).
[28] A. Cheek, L. Heurtier, Y. F. Perez-Gonzalez, and J. Turner, arXiv:2107.00016.
[29] A. Cheek, L. Heurtier, Y. F. Perez-Gonzalez, and J. Turner, arXiv:2107.00013.
[30] B. Barman, D. Borah, S. J. Das, and R. Roshan, J. Cosmol. Astropart. Phys. 03 (2022) 031.
[31] D. Borah, S. Jyoti Das, R. Samanta, and F. R. Urban, J. High Energy Phys. 03 (2023) 127.
[32] M. Chen, G. B. Gelmini, P. Lu, and V. Takhistov, arXiv: 2309.12258.
[33] M. Chen, G. B. Gelmini, P. Lu, and V. Takhistov, arXiv: 2312.12136.
[34] T. Kim, P. Lu, D. Marfatia, and V. Takhistov, arXiv: 2309.05703.
[35] T. C. Gehrman, B. Shams Es Haghi, K. Sinha, and T. Xu, arXiv:2310.08526.
[36] B. J. Carr, Astrophys. J. **206**, 8 (1976).
[37] D. Baumann, P. J. Steinhardt, and N. Turok, arXiv:hep-th/0703250.
[38] A. Hook, Phys. Rev. D **90**, 083535 (2014).
[39] T. Fujita, M. Kawasaki, K. Harigaya, and R. Matsuda, Phys. Rev. D **89**, 103501 (2014).
[40] Y. Hamada and S. Iso, Prog. Theor. Exp. Phys. **2017**, 033B02 (2017).
[41] D. Hooper and G. Krnjaic, Phys. Rev. D **103**, 043504 (2021).
[42] Y. F. Perez-Gonzalez and J. Turner, Phys. Rev. D **104**, 103021 (2021).
[43] S. Datta, A. Ghosal, and R. Samanta, J. Cosmol. Astropart. Phys. 08 (2021) 021.
[44] S. Jyoti Das, D. Mahanta, and D. Borah, J. Cosmol. Astropart. Phys. 11 (2021) 019.
[45] N. Smyth, L. Santos-Olmsted, and S. Profumo, arXiv:2110.14660.
[46] N. Bernal, C. S. Fong, Y. F. Perez-Gonzalez, and J. Turner, arXiv:2203.08823.
[47] A. Ambrosone, R. Calabrese, D. F. G. Fiorillo, G. Miele, and S. Morisi, Phys. Rev. D **105**, 045001 (2022).
[48] R. Calabrese, M. Chianese, J. Gunn, G. Miele, S. Morisi, and N. Saviano, Phys. Rev. D **107**, 123537 (2023).
[49] R. Calabrese, M. Chianese, J. Gunn, G. Miele, S. Morisi, and N. Saviano, arXiv:2311.13276.
[50] T. C. Gehrman, B. Shams Es Haghi, K. Sinha, and T. Xu, J. Cosmol. Astropart. Phys. 02 (2023) 062.
[51] T. C. Gehrman, B. Shams Es Haghi, K. Sinha, and T. Xu, J. Cosmol. Astropart. Phys. 10 (2023) 001.
[52] C. Lunardini and Y. F. Perez-Gonzalez, J. Cosmol. Astropart. Phys. 08 (2020) 014.
[53] F. Schiavone, D. Montanino, A. Mirizzi, and F. Capozzi, J. Cosmol. Astropart. Phys. 08 (2021) 063.
[54] N. Bernal, V. Muñoz Albornoz, S. Palomares-Ruiz, and P. Villanueva-Domingo, arXiv:2203.14979.
[55] B. Barman, D. Borah, S. Jyoti Das, and R. Roshan, Phys. Rev. D **107**, 095002 (2023).
[56] A. Datta, R. Roshan, and A. Sil, Phys. Rev. Lett. **132**, 061802 (2024).
[57] A. Datta, R. Roshan, and A. Sil, Phys. Rev. D **108**, 035029 (2023).
[58] M. Riajul Haque, E. Kpatcha, D. Maity, and Y. Mambrini, Phys. Rev. D **108**, 063523 (2023).
[59] M. R. Haque, E. Kpatcha, D. Maity, and Y. Mambrini, Phys. Rev. D **109**, 023521 (2024).
[60] M. Fukugita and T. Yanagida, Phys. Lett. **174B**, 45 (1986).
[61] S. Davidson, E. Nardi, and Y. Nir, Phys. Rep. **466**, 105 (2008).
[62] V. A. Kuzmin, V. A. Rubakov, and M. E. Shaposhnikov, Phys. Lett. **155B**, 36 (1985).
[63] W. Buchmuller, P. Di Bari, and M. Plumacher, Nucl. Phys. **B643**, 367 (2002); **B793**, 362(E) (2008).
[64] W. Buchmuller, P. Di Bari, and M. Plumacher, Nucl. Phys. **B665**, 445 (2003).
[65] P. H. Chankowski and K. Turzynski, Phys. Lett. B **570**, 198 (2003).
[66] G. Giudice, A. Notari, M. Raidal, A. Riotto, and A. Strumia, Nucl. Phys. **B685**, 89 (2004).
[67] S. Davidson and A. Ibarra, Phys. Lett. B **535**, 25 (2002).
[68] S. Weinberg, Phys. Rev. Lett. **48**, 1303 (1982).
[69] G. Giudice, M. Peloso, A. Riotto, and I. Tkachev, J. High Energy Phys. 08 (1999) 014.
[70] T. Asaka, K. Hamaguchi, M. Kawasaki, and T. Yanagida, Phys. Lett. B **464**, 12 (1999).
[71] G. Lazarides and Q. Shafi, Phys. Lett. B **258**, 305 (1991).
[72] B. A. Campbell, S. Davidson, and K. A. Olive, Nucl. Phys. **B399**, 111 (1993).
[73] F. Hahn-Woernle and M. Plumacher, Nucl. Phys. **B806**, 68 (2009).
[74] B. Barman, D. Borah, and R. Roshan, Phys. Rev. D **104**, 035022 (2021).
[75] S. Y. Choi, J. S. Shim, and H. S. Song, Phys. Rev. D **51**, 2751 (1995).
[76] B. R. Holstein, Am. J. Phys. **74**, 1002 (2006).
[77] R. T. Co, Y. Mambrini, and K. A. Olive, arXiv:2205.01689.
[78] B. Barman, S. Cléry, R. T. Co, Y. Mambrini, and K. A. Olive, J. High Energy Phys. 12 (2022) 072.
[79] S. Clery, Y. Mambrini, K. A. Olive, and S. Verner, Phys. Rev. D **105**, 075005 (2022).
[80] M. R. Haque and D. Maity, Phys. Rev. D **107**, 043531 (2023).

[81] S. Clery, Y. Mambrini, K. A. Olive, A. Shkerin, and S. Verner, Phys. Rev. D **105**, 095042 (2022).
[82] M. R. Haque, D. Maity, and R. Mondal, arXiv:2311.07684.
[83] R. Roshan and G. White, arXiv:2401.04388.
[84] M. Giovannini, Phys. Rev. D **58**, 083504 (1998).
[85] M. Giovannini, Phys. Rev. D **60**, 123511 (1999).
[86] A. Riazuelo and J.-P. Uzan, Phys. Rev. D **62**, 083506 (2000).
[87] N. Seto and J. Yokoyama, J. Phys. Soc. Jpn. **72**, 3082 (2003).
[88] L. A. Boyle and A. Buonanno, Phys. Rev. D **78**, 043531 (2008).
[89] A. Stewart and R. Brandenberger, J. Cosmol. Astropart. Phys. 08 (2008) 012.
[90] B. Li and P. R. Shapiro, J. Cosmol. Astropart. Phys. 10 (2021) 024.
[91] M. Artymowski, O. Czerwinska, Z. Lalak, and M. Lewicki, J. Cosmol. Astropart. Phys. 04 (2018) 046.
[92] C. Caprini and D. G. Figueroa, Classical Quantum Gravity **35**, 163001 (2018).
[93] D. Bettoni, G. Domènech, and J. Rubio, J. Cosmol. Astropart. Phys. 02 (2019) 034.
[94] N. Bernal and F. Hajkarim, Phys. Rev. D **100**, 063502 (2019).
[95] D. G. Figueroa and E. H. Tanin, J. Cosmol. Astropart. Phys. 08 (2019) 011.
[96] T. Opferkuch, P. Schwaller, and B. A. Stefanek, J. Cosmol. Astropart. Phys. 07 (2019) 016.
[97] N. Bernal, A. Ghoshal, F. Hajkarim, and G. Lambiase, arXiv:2008.04959.
[98] A. Ghoshal, L. Heurtier, and A. Paul, J. High Energy Phys. 12 (2022) 105.
[99] R. Caldwell *et al.*, Gen. Relativ. Gravit. **54**, 156 (2022).
[100] Y. Gouttenoire, G. Servant, and P. Simakachorn, arXiv:2111.01150.
[101] B. Barman, A. Ghoshal, B. Grzadkowski, and A. Socha, J. High Energy Phys. 07 (2023) 231.
[102] A. Chakraborty, M. R. Haque, D. Maity, and R. Mondal, Phys. Rev. D **108**, 023515 (2023).
[103] B. Barman and A. Datta, arXiv:2312.13821.
[104] J. Crowder and N. J. Cornish, Phys. Rev. D **72**, 083005 (2005).
[105] V. Corbin and N. J. Cornish, Classical Quantum Gravity **23**, 2435 (2006).
[106] S. Kawamura *et al.*, Classical Quantum Gravity **23**, S125 (2006).
[107] S. Kawamura *et al.*, Prog. Theor. Exp. Phys. **2021**, 05A105 (2021).
[108] B. J. Carr and S. W. Hawking, Mon. Not. R. Astron. Soc. **168**, 399 (1974).
[109] J. H. MacGibbon and B. R. Webber, Phys. Rev. D **41**, 3052 (1990).
[110] J. Auffinger, I. Masina, and G. Orlando, Eur. Phys. J. Plus **136**, 261 (2021).
[111] K. Kaneta, Y. Mambrini, K. A. Olive, and S. Verner, Phys. Rev. D **101**, 015002 (2020).
[112] M. A. G. Garcia, K. Kaneta, Y. Mambrini, and K. A. Olive, Phys. Rev. D **101**, 123507 (2020).
[113] M. A. G. Garcia, K. Kaneta, Y. Mambrini, and K. A. Olive, J. Cosmol. Astropart. Phys. 04 (2021) 012.
[114] P. B. Greene and L. Kofman, Phys. Lett. B **448**, 6 (1999).
[115] L. A. Boyle and P. J. Steinhardt, Phys. Rev. D **77**, 063504 (2008).
[116] Y. Watanabe and E. Komatsu, Phys. Rev. D **73**, 123515 (2006).
[117] K. Saikawa and S. Shirai, J. Cosmol. Astropart. Phys. 05 (2018) 035.
[118] S. S. Mishra, V. Sahni, and A. A. Starobinsky, J. Cosmol. Astropart. Phys. 05 (2021) 075.
[119] M. R. Haque, D. Maity, T. Paul, and L. Sriramkumar, Phys. Rev. D **104**, 063513 (2021).
[120] T. Papanikolaou, V. Vennin, and D. Langlois, J. Cosmol. Astropart. Phys. 03 (2021) 053.
[121] G. Domènech, C. Lin, and M. Sasaki, J. Cosmol. Astropart. Phys. 04 (2021) 062; 11 (2021) E01.
[122] G. Domènech, V. Takhistov, and M. Sasaki, Phys. Lett. B **823**, 136722 (2021).
[123] G. Domènech, Universe **7**, 398 (2021).
[124] B. P. Abbott *et al.* (LIGO Scientific and Virgo Collaborations), Phys. Rev. Lett. **116**, 061102 (2016).
[125] B. P. Abbott *et al.* (LIGO Scientific and Virgo Collaborations), Phys. Rev. Lett. **116**, 241103 (2016).
[126] B. P. Abbott *et al.* (LIGO Scientific and Virgo Collaborations), Phys. Rev. Lett. **118**, 221101 (2017); **121**, 129901 (E) (2018).
[127] B. P. Abbott *et al.* (LIGO Scientific and Virgo Collaborations), Astrophys. J. Lett. **851**, L35 (2017).
[128] B. P. Abbott *et al.* (LIGO Scientific and Virgo Collaborations), Phys. Rev. Lett. **119**, 141101 (2017).
[129] B. P. Abbott *et al.* (LIGO Scientific and Virgo Collaborations), Phys. Rev. Lett. **119**, 161101 (2017).
[130] P. Amaro-Seoane *et al.* (LISA Collaboration), arXiv:1702.00786.
[131] J. Baker *et al.*, arXiv:1907.06482.
[132] B. P. Abbott *et al.* (LIGO Scientific Collaboration), Classical Quantum Gravity **34**, 044001 (2017).
[133] D. Reitze *et al.*, Bull. Am. Astron. Soc. **51**, 035 (2019), arXiv:1907.04833.
[134] M. Punturo *et al.*, Classical Quantum Gravity **27**, 194002 (2010).
[135] S. Hild *et al.*, Classical Quantum Gravity **28**, 094013 (2011).
[136] N. Seto, S. Kawamura, and T. Nakamura, Phys. Rev. Lett. **87**, 221103 (2001).
[137] H. Kudoh, A. Taruya, T. Hiramatsu, and Y. Himemoto, Phys. Rev. D **73**, 064006 (2006).
[138] K. Nakayama and J. Yokoyama, J. Cosmol. Astropart. Phys. 01 (2010) 010.
[139] K. Yagi and N. Seto, Phys. Rev. D **83**, 044011 (2011); **95**, 109901(E) (2017).
[140] A. Sesana *et al.*, Exper. Astron. **51**, 1333 (2021).
[141] K. Schmitz, arXiv:2002.04615.
[142] A. Ringwald, J. Schütte-Engel, and C. Tamarit, J. Cosmol. Astropart. Phys. 03 (2021) 054.
[143] A. Ringwald and C. Tamarit, Phys. Rev. D **106**, 063027 (2022).
[144] S. Dodelson and M. S. Turner, Phys. Rev. D **46**, 3372 (1992).
[145] S. Hannestad and J. Madsen, Phys. Rev. D **52**, 1764 (1995).

[146] A. D. Dolgov, S. H. Hansen, and D. V. Semikoz, Nucl. Phys. **B503**, 426 (1997).
[147] G. Mangano, G. Miele, S. Pastor, T. Pinto, O. Pisanti, and P. D. Serpico, Nucl. Phys. **B729**, 221 (2005).
[148] P. F. de Salas and S. Pastor, J. Cosmol. Astropart. Phys. 07 (2016) 051.
[149] M. Escudero Abenza, J. Cosmol. Astropart. Phys. 05 (2020) 048.
[150] K. Akita and M. Yamaguchi, J. Cosmol. Astropart. Phys. 08 (2020) 012.
[151] J. Froustey, C. Pitrou, and M. C. Volpe, J. Cosmol. Astropart. Phys. 12 (2020) 015.
[152] J. J. Bennett, G. Buldgen, P. F. De Salas, M. Drewes, S. Gariazzo, S. Pastor, and Y. Y. Y. Wong, J. Cosmol. Astropart. Phys. 04 (2021) 073.
[153] M. Maggiore, Phys. Rep. **331**, 283 (2000).
[154] M. Kawasaki, K. Kohri, and N. Sugiyama, Phys. Rev. Lett. **82**, 4168 (1999).
[155] M. Kawasaki, K. Kohri, and N. Sugiyama, Phys. Rev. D **62**, 023506 (2000).
[156] T. Hasegawa, N. Hiroshima, K. Kohri, R. S. L. Hansen, T. Tram, and S. Hannestad, J. Cosmol. Astropart. Phys. 12 (2019) 012.
[157] T.-H. Yeh, J. Shelton, K. A. Olive, and B. D. Fields, arXiv:2207.13133.
[158] K. Abazajian *et al.*, arXiv:1907.04473.
[159] S. Aiola *et al.* (CMB-HD Collaboration), arXiv:2203.05728.
[160] F. R. Bouchet *et al.* (COrE Collaboration), arXiv:1102.2181.
[161] R. Laureijs *et al.* (EUCLID Collaboration), arXiv:1110.3193.
[162] S. Hanany *et al.* (NASA PICO Collaboration), arXiv:1902.10541.
[163] M. Gell-Mann, P. Ramond, and R. Slansky, Conf. Proc. C **790927**, 315 (1979), arXiv:1306.4669.
[164] R. N. Mohapatra and G. Senjanovic, Phys. Rev. Lett. **44**, 912 (1980).
[165] P. Minkowski, Phys. Lett. **67B**, 421 (1977).
[166] P. A. Zyla *et al.* (Particle Data Group), Prog. Theor. Exp. Phys. **2020**, 083C01 (2020).
[167] J. A. Casas and A. Ibarra, Nucl. Phys. **B618**, 171 (2001).
[168] R. Kallosh and A. Linde, J. Cosmol. Astropart. Phys. 07 (2013) 002.
[169] R. Kallosh, A. Linde, and D. Roest, J. High Energy Phys. 11 (2013) 198.
[170] Y. Akrami *et al.* (Planck Collaboration), Astron. Astrophys. **641**, A10 (2020).